NATIONAL ADVISORY COMMITTEE FOR AERONAUTICS

TECHNICAL NOTE 3097

TURBULENT BOUNDARY-LAYER AND SKIN-FRICTION MEASUREMENTS IN AXIAL FLOW ALONG CYLINDERS AT MACH NUMBERS BETWEEN 0.5 AND 3.6

By Dean R. Chapman and Robert H. Kester

Ames Aeronautical Laboratory
Moffett Field, Calif.

NACA

Washington
March 1954

NATIONAL ADVISORY COMMITTEE FOR AERONAUTICS

TECHNICAL NOTE 3097

TURBULENT BOUNDARY-LAYER AND SKIN-FRICTION MEASUREMENTS IN AXIAL FLOW ALONG CYLINDERS AT MACH NUMBERS BETWEEN 0.5 AND 3.6

By Dean R. Chapman and Robert H. Kester

SUMMARY

Experiments have been conducted to determine average skin-friction coefficients in the absence of heat transfer for completely turbulent flow along the cylindrical portion of cone-cylinder bodies of revolution having over-all fineness ratios of 10, 15, and 25. The friction data were obtained by directly measuring forces. Numerous boundary-layer surveys were made to enable all data to be based on an effective starting position of the turbulent flow. Mach numbers of 0.5, 0.8, 2.0, 2.5, 2.9, 3.4, and 3.6, and Reynolds numbers between 4 million and 32 million were investigated. At a Mach number of 2.0, data were obtained for different pressure distributions by distorting the flexible-plate walls of the wind tunnel.

The results show no significant effect on average skin-friction coefficient of small changes in pressure gradient. At both subsonic and supersonic velocities, the skin-friction coefficient depends only to a small extent on cylinder length-diameter ratio. For each length-diameter ratio, however, the effect of Mach number is large, amounting to approximately a 50-percent reduction in skin-friction coefficient as the Mach number is increased from 0 to 4. This effect of Mach number does not depend significantly on Reynolds number or cylinder fineness ratio.

Comparison with similar experiments on flat plates, primarily those of Coles, shows good agreement as to the effect of Mach number on skin friction, although the velocity profiles measured on cylinders are appreciably different from those on a flat plate. Determinations of friction by the momentum method differed considerably from the more reliable direct-force measurements.

INTRODUCTION

One of the interesting aspects of average skin-friction measurements for turbulent boundary layers is the unusually extensive history of experiments conducted in this field. A comprehensive survey of the numerous experiments may be found, for example, in the often-cited paper of

Schoenherr (ref. 1) which covered measurements prior to 1932. More recent surveys by Locke (ref. 2) and Hughes (ref. 3) have covered measurements made in the subsequent 20 years. An accurate knowledge of skin friction for turbulent incompressible flow has, of course, long been of concern in the field of naval architecture, with the result that measurements of surface skin friction date at least as far back as some experiments of Beaufoy conducted near the end of the 18th century. When these early data are reduced to dimensionless coefficient form and plotted as a function of Reynolds number, the resulting agreement with recent measurements is surprisingly good. (See refs. 1 and 2.)

Theoretical investigations of skin friction for turbulent flow, on the other hand, are of comparatively recent origin. It is well known that the semiempirical mixing-length analyses of von Kármán and Prandtl, advanced approximately 20 years ago, yield fairly accurate predictions of turbulent friction for a flat plate in low-speed flow. Interestingly enough, though, subsequent detailed hot-wire measurements, such as those of Liepmann and Laufer (ref. 4) and Townsend (ref. 5), have indicated the fundamental mixing-length hypothesis to be incorrect. The good agreement between predicted skin friction and experiment can be attributed in considerable part to the fact that mixing-length analyses yield arbitrary constants of integration which are free to be adjusted by comparison with experiment. With constants empirically determined from friction measurements, the corresponding velocity profiles predicted by mixing-length theory using these same constants do not agree well with measurements except over a limited portion of the boundary layer. This was noted by Gurjienko (ref. 6) and is apparent in almost all measurements dating from those of Schultz-Grunow (ref. 7) up to the most recent and detailed measurements of Klebanoff (ref. 8).

The most satisfactory analytical treatment of the low-speed turbulent boundary layer on a flat plate does not utilize mixing-length suppositions, but combines instead two empirical laws concerning the similarity of velocity profiles: the so-called "wall" law which was formulated by Prandtl, as noted in reference 9, and the so-called "velocity-decrement" law which was first observed for pipe flow by Darcy almost 100 years ago (ref. 10), then rediscovered by Stanton (ref. 11) for pipe flow, and later observed by Fritsch (ref. 12) for channel flow. For the special case of boundary-layer flow of an incompressible fluid along a flat plate, the analytical exploitation of these two similarity laws to predict skin friction and other important turbulent boundary-layer characteristics was initially given by Kármán (ref. 13). The fundamental basis of this velocity-profile similarity method, which is totally different in principle from the mixing-length method of Kármán, has been discussed by Millikan in reference 14. A detailed review of the combined wall law and velocity-decrement law, including utilization of the equations of motion to calculate the shear-stress distribution across the boundary layer, may be found in the recent thesis of Coles (ref. 15).

An active interest of aerodynamicists in the basic knowledge of turbulent boundary layers has been revived because of the necessity of extending methods of predicting incompressible boundary-layer characteristics to high Mach numbers where large variations in density occur across the boundary layer. Similarity laws for the variation of mean properties across a turbulent boundary layer in compressible flow have not as yet been found, although Coles has formulated a generalization of the wall law which involves an unknown function of Mach number to be determined from experiments. In the absence of detailed experiments to provide a sound foundation for analysis, recourse to mixing-length calculations and similar unproven hypotheses has been made in the past by a number of investigators in an attempt to obtain information about the turbulent boundary layer at high Mach numbers. The results, unfortunately, have been almost as varied as the number of investigators. This is indicated by figure 1 which shows the results (see refs. 16 to 31) of various theoretical analyses of skin friction on an insulated plate in compressible turbulent flow.[1] Since a brief discussion of these analyses was provided in a summary report of the present research (ref. 36) and also may be found in more detail in Coles' thesis (ref. 15), no further discussion is given here. It will suffice, instead, to emphasize only what is clearly indicated by figure 1; namely, the present theoretical knowledge of turbulent boundary layers in compressible flow is severely limited.

The practical reasons for requiring detailed knowledge of turbulent skin friction at high Mach numbers are twofold. The first concerns the obvious direct application to drag and, hence, performance estimations. The second, which is becoming of increasing practical importance, concerns the application to heat-transfer calculations, or the so-called "aerodynamic heating" problem. Although various estimates of heat-transfer rate (see Rubesin's compilation in ref. 37 or the compilation of curves in ref. 36) are about equally as varied as those of skin friction, they, nevertheless, have one characteristic in common: a calculation of heat transfer first requires a knowledge of skin friction. Average skin-friction measurements can be used directly to estimate average heat-transfer rates for conditions of constant surface temperature. Such measurements also can be used indirectly as a guide in estimating local skin friction and local heat transfer, the two fundamental quantities used in practical calculations for conditions of variable surface temperature and pressure.

In cognizance of the limitations of present turbulence theory and the necessity of knowing skin friction before either drag or heat transfer

[1]Not indicated on this plot are the results of Dorodnitsyn (ref. 32) and and Kalikhman (ref. 33) which coincide with Kármán's estimation, and the result of Tetervin (ref. 34) which predicts no effect of compressibility. Also not shown are the "power-law generalization" of Cope (ref. 18) which is tedious to compute at high Mach numbers because of poor series convergence, and the analysis of Donaldson (ref. 35) which apparently was not carried far enough to predict the effect of Mach number for constant-length Reynolds number.

can be estimated, numerous measurements of turbulent skin friction in compressible flow have been made during the last few years. In this connection, reference is made to the measurements of Wilson (ref. 21); Rubesin, Maydew, and Varga (ref. 25); Liepmann and Dhawan (ref. 28); Coles (refs. 15 and 39); Brinich and Diaconis (ref. 40); Bradfield, DeCoursin, and Blumer (ref. 41); Cope (ref. 42); Weiler and Hartwig (ref. 43); Spivack (ref. 44); Monaghan and Johnson (ref. 45); Ladenburg and Bershader (ref. 46); Bloom (ref. 47); and Hakkinen (ref. 48). Results of these measurements are discussed later, especially those of Coles.

The purpose of the present investigation was to measure the average friction for turbulent flow along the external surface of relatively long cylindrical bodies of revolution at both supersonic and subsonic speeds. For long cylinders the boundary-layer thickness becomes comparable to the cylinder radius, under which conditions appreciable departures from flat-plate skin-friction values would be expected, according to the analyses of Jakob and Dow (ref. 49), Landweber (ref. 50), and Eckert (ref. 51). Consequently, in the present tests various cylinders were investigated ranging in length from 8 to 23 diameters. The inclusion of subsonic measurements as an integral part of the investigation was believed necessary for an accurate evaluation of the effect of Mach number, since adequate skin-friction data were not available for incompressible flow along cylinders. It was considered desirable, further, to determine the friction by measuring forces directly, rather than to deduce the friction indirectly from boundary-layer surveys according to the momentum method. As will be seen later, these two features proved quite valuable in minimizing several uncertainties common to most previous investigations.

The present experiments were initiated in 1949, though the technique of measurement finally employed was not developed satisfactorily until a year later. The data presented herein were obtained during 1950-52. Some of the principal results have been summarized previously in reference 36.

NOTATION

C_F average skin-friction coefficient, $\dfrac{\text{force}}{(1/2)\rho_\infty u_\infty^2 \text{ (wetted area)}}$

c_f local skin-friction coefficient, $\dfrac{2\tau_w}{\rho_\infty u_\infty^2}$

D cylinder diameter

f friction force on cylinder of length l

Δf friction force on cylinder of length Δl

l length of cylinder over which friction force was measured

Δl length of cylinder necessary to produce boundary layer of momentum thickness θ_o at Reynolds number, $\frac{U_o \Delta l}{\nu_o}$

L corrected length of cylinder, $l+\Delta l$

M Mach number

p static pressure

p_b base pressure (average of readings from five orifices)

p_t' total pressure behind normal shock wave

Re Reynolds number

R_θ Reynolds number based on momentum thickness

T temperature

u velocity

y distance from surface

δ boundary-layer thickness

θ boundary-layer momentum thickness for cylinder,

$$\int_o^\infty \frac{\rho u}{\rho_e u_e}\left(1 - \frac{u}{u_e}\right)\left(1 + \frac{2y}{D}\right) dy$$

μ coefficient of viscosity

ν kinematic viscosity, $\frac{\mu}{\rho}$

ρ mass density

τ_w shear stress at wall

Subscripts

i incompressible flow

o conditions at station 0 (See fig. 2 and table I.)

e local conditions at outer edge of boundary layer

∞ average of conditions at outer edge of boundary layer over length L

w conditions at wall

t total conditions

APPARATUS AND TEST METHODS

Wind Tunnels

Tests were conducted in the Ames 1- by 3-foot supersonic wind tunnels No. 1 and No. 2. Wind tunnel No. 1 is of the closed-circuit, continuous-operation type equipped with a flexible-plate nozzle that provides a variation of Mach number from 1.2 to 2.2. Total pressure in tunnel No. 1 can be varied to provide Reynolds numbers from 1 million to 10 million per foot. Wind tunnel No. 2 is of the nonreturn, intermittent-operation type also equipped with a flexible-plate nozzle to provide a variation of Mach number from 0.5 to 3.8. Compressed air at a maximum pressure of 6 atmospheres is obtained from a reservoir and is expanded through the nozzle to atmospheric pressure. The total pressure is controlled by means of a throttling butterfly valve between the reservoir and the tunnel settling chamber, providing a variation of Reynolds number from 7 million to 20 million per foot.

Primarily because of the throttling method employed, the tunnel turbulence level in the No. 2 tunnel is much higher than that in the No. 1 tunnel. Some unpublished hot-wire measurements made by Howard A. Stine of the NACA Ames Laboratory have indicated the turbulence level in the No. 1 tunnel to be between 2 and 3 percent as measured in the reservoir at a location where the velocity was of the order of 15 feet per second. In the one-year interval between the last of the skin-friction measurements and these recent hot-wire measurements, the No. 2 tunnel was completely revised. Consequently, recent hot-wire measurements in the No. 2 tunnel, which indicate the turbulence level at the time of this writing to be between 2 and 10 percent, depending on operating conditions of total pressure and Mach number, do not apply to data presented in this report. As a result of the revisions, though, it is known that the transition Reynolds number on a 10° cone (measured by the method described in ref. 52) was increased several fold. It is believed, therefore, that the turbulence level for the No. 2 tunnel as it existed during the skin-friction measurements was considerably greater than that for the revised tunnel. It will be shown later that the difference in turbulence levels of the two wind tunnels had no measureable effect on turbulent skin friction at a Mach number of 2.

The water content of the air in both wind tunnels was maintained at less than 0.0003 pound of water per pound of dry air. Consequently, no correction was made for humidity effects.

Force Measurements

The friction force f acting along a cylinder of length l and diameter D was determined from two drag measurements by subtracting the absolute foredrag (sum of measured drag force and the product $p_b\pi D^2/4$) of a short cone-cylinder of length l' from that of a much longer cone-cylinder of length $l+l'$. (See fig. 2.) Photographs of two models employed are shown in figure 3. Models were anodize-finished aluminum and appear black in the photographs as contrasted with the cadmium-plated shrouds. For each model the cylinder diameter was 1 inch and the included cone angle was 20°. Three different lengths $l+l'$ were investigated: 10, 15, and 25 inches, as measured from the tip of cone to base of cylinder. In the final C_F data to be discussed below, these lengths corresponded to cylinder fineness ratios of approximately 8, 13, and 23, respectively. It was found necessary to provide boundary-layer trips in order to assure a turbulent boundary layer in all but a few test conditions. The trips employed will be discussed later. The magnitude of the friction drag was between 20 percent and 50 percent of the over-all body drag and is believed to have been measured with a corresponding accuracy of from 4 percent to 2 percent, depending upon length-diameter ratio and test conditions.

Total drag was measured by means of a three-component electrical-strain-gage balance which had been specially adapted to the measurement of axial force for the present investigation. The balance and supporting stings were shielded from the oncoming flow by shrouds in the manner shown by the photograph of figure 3. The cylinders were alined with the shrouds by the use of ball-bearing guides through which the stings were passed.

Base drag was measured by means of five base-pressure orifices connected to a multimanometer using dibutal phthalate as the manometer fluid. Three of these orifices were located evenly spaced in the face of each shroud, the fourth being located on the sting, and the fifth inside the balance chamber. In addition to determining the base drag, the five pressure measurements provided a sensitive indication of alinement of cone-cylinders with shrouds and also confirmed the absence of leaks in the balance-shroud enclosure. No data were taken unless the five base pressures were in essential agreement. A reference tube of the manometer was connected to a vacuum pump during supersonic testing but was left open to the atmosphere when operating at subsonic speeds. A McLeod gage was used to measure the pressure of the vacuum reference.

Apexes of the two cone-cylinders needed for one friction-force measurement were made to occupy the same position in the tunnel test section, thereby eliminating the need of an axial buoyancy correction. This technique also enabled axial pressure distribution along the cylinder over which the friction force acted to be measured by eight equally spaced orifices located in that portion of the shroud surface which corresponded to the cylinder of length l. Static-pressure distributions obtained in this manner were found to agree with those measured on a similar cone-cylinder model without a gap.

Allowance was made for the fact that the two drag measurements used in determining the friction force f were made during two separate runs under slightly different conditions of tunnel pressure and temperature. Faired curves of the absolute foredrag coefficient of the short cone-cylinder plotted against Reynolds number per unit length were used to determine the absolute foredrag at the particular Reynolds number corresponding to the drag measurement of the long cone-cylinder.

The drag gage was calibrated prior to each day's testing, and a check of the balance was made before and after each test to assure that the friction in the balance system was negligible while measuring forces. This practice showed that periodic cleaning of the balance was essential to the satisfactory measurement of the friction force. Further uncertainties were minimized by repeating each set of measurements at least once.

Method of Determining Effective Reynolds Number and Corrected Skin-Friction Coefficient

As indicated in the center sketch of figure 2, the boundary-layer thickness at the leading edge of the cylinder over which the friction force f was measured was not zero but some value δ_o. Hence, to provide a common basis of comparison, it was necessary to apply corrections in order to convert the force measurements to conditions of completely turbulent flow starting with zero boundary-layer thickness at the leading edge of a cylinder. For this purpose one can imagine the cylindrical surface to be extended upstream a short distance Δl (see bottom sketch in fig. 2) such that the turbulent boundary-layer momentum thickness developed over the length Δl just matches the momentum thickness θ_o corresponding to the boundary-layer thickness δ_o. Boundary-layer surveys in the plane of station 0, as illustrated in the sketch second from the bottom in figure 2, were used to determine boundary-layer profiles from which Δl and the corresponding friction force Δf were calculated. The surveys showed that θ_o depended on M_∞, Re, nose shape, etc., in a complicated manner that could be determined only by measurement. As a result, it was necessary to obtain boundary-layer surveys in this position for all the conditions under which the direct-force measurements were obtained. This proved to be a time-consuming task since it involved

making a total of about 270 boundary-layer surveys. The small friction force Δf that would act over the length Δl was readily determined from the equation

$$\Delta f = \pi D \rho_o u_o^2 \theta_o$$

which represents conservation of momentum. The length Δl was determined from an equivalent form of the momentum equation

$$\Delta l = \frac{2\theta_o}{C_{F_o}}$$

Actually, the skin-friction coefficient C_{F_o}, based on the Reynolds number $u_o \Delta l / \nu_o$, was not known until Δl was known. Hence, the method of determining C_{F_o} and Δl was, in principle, an iterative one, using the equation

$$C_{F_o} = C_{F_{io}} \left(\frac{C_F}{C_{F_i}} \right)$$

with $C_{F_{io}}$ evaluated at a Reynolds number $u_o \Delta l / \nu_o$ from the Kármán-Schoenherr equation

$$\frac{0.242}{\sqrt{C_{F_i}}} = \log_{10} (\mathrm{Re} C_{F_i})$$

in conjunction with the ratio (C_F/C_{F_i}) evaluated at an arbitrary Reynolds number from a plot of uncorrected force data (this latter ratio does not depend significantly on Reynolds number). It turned out that the corrections Δl and Δf were sufficiently small and the correction method so rapidly convergent, that, after the first few trials, iteration was found to be unnecessary.

The average skin-friction coefficient C_F and corresponding Reynolds number Re employed throughout are based on the total length $L = l + \Delta l$ and the total force $f + \Delta f$ according to the defining equations

$$C_F = \frac{f + \Delta f}{(1/2)\, \rho_\infty u_\infty^2 [\pi D (l + \Delta l)]}$$

$$\mathrm{Re} = \frac{U_\infty (l + \Delta l)}{\nu_\infty}$$

Reference quantities such as M_∞, ρ_∞, u_∞, and ν_∞ correspond to conditions at the outer edge of the boundary layer averaged over the length L. These were determined from measurements of total pressure, static pressure,

total temperature, and the Sutherland equation for viscosity (with $S = 216^{\circ}$ R and $\mu = 0.361 \times 10^{-6}$ lb sec ft^{-2} at 500° R), assuming the air to be a perfect gas.

Since it is not possible in any experiment to obtain fully developed turbulent flow starting precisely at the leading edge, some assumption inevitably is involved in any method of determining the effective starting position of turbulence, even though the method appears to be based on measured quantities such as momentum thickness. The method described above is based on the assumption that the ratio C_F/C_{F_i} does not depend significantly on Reynolds number. This assumption should be reasonable for the Reynolds numbers of the investigation. (The lowest Reynolds number at which the starting-length correction was applied was 0.4×10^6.) Other methods have been employed which involve different assumptions (see refs. 15, 21, 25, 45, and 46). None of the methods is exact. Hence, in order to obtain accurate and consistent data, it is necessary that the starting-length correction be sufficiently small so that various correction methods would yield substantially the same end result. Such conditions were met in the present experiments inasmuch as the starting-length correction to skin-friction coefficient was relatively small. This correction generally decreased with increasing Mach number, varying between 10 and 3 percent for $L/D = 8$, 6 and 2 percent for $L/D = 13$, and 4 and 1 percent for $L/D = 23$. In the most extreme case, a 10-percent error in the correction itself would introduce 1-percent error in C_F.

Boundary-Layer Survey Apparatus and Reduction of Survey Data

The apparatus used in obtaining all survey measurements is shown in the photograph of figure 4 which illustrates the position of the various components of the equipment while making boundary-layer surveys in the plane of station 0. Dimensions locating this station, as well as the other stations at which surveys were made, are given in table I. The survey instrument consisted essentially of a housing pinned to a supporting member. A boundary-layer probe which was attached to the housing could be moved in a vertical direction since the housing could be rotated approximately 2° in the vertical plane passing through the tunnel axis. Because the probe opening was located about 15 inches upstream of the pivot pin, the probe mouth could be considered to move in a straight line. Motion was provided by the use of an electric motor located outside the wind tunnel and connected to the survey instrument by a flexible shaft. Speed reduction was such that position in the vertical direction could be controlled to about 0.0005 inch.

Two probes were used, the dimensions of which are given in the table of figure 5. These probes were constructed of stainless-steel hypodermic tubing following the spirit of the suggestions of reference 53. Time lags of the order of 5 seconds for the highest Mach number and a fraction of a second for the lowest Mach number were obtained.

Probe-opening position and pitot pressure were determined by an electrical-resistance strain gage and a pressure cell, respectively, both of which were located within the instrument housing. The base of the strain gage was fixed to the supporting member in such a manner that deflection of the gage was increased by downward movement of the housing. Characteristics of the pressure cell employed can be found in reference 54. Static pressure was determined (with the probe outside the boundary layer) by means of orifices located in the surface of the survey model at the various boundary-layer survey stations. At each station two orifices were located in a vertical plane on opposite sides of the model from each other in order to indicate the degree to which the model had been alined with the stream. This precaution, however, did not assure obtaining identical boundary-layer surveys from the top and bottom of the survey model except in a few cases due to the high sensitivity of boundary-layer profile to small stream angles.

Two methods were used to determine the point at which the probe contacted the surface of the survey model in wind tunnel No. 1. Since the survey model was electrically insulated from the survey instrument, the point at which contact occurred should have been indicated by a marked decrease in the resistance between probe and model as measured by an electrical analyzer. Actually, either the probe or the model vibrated somewhat so that approaching contact was at first indicated by intermittent indications of the meter and, as the probe continued toward the model, the mean value of the indicated resistance steadily decreased until solid contact was finally made. In order to determine the value of the resistance which corresponded to effective probe contact, the region near contact was viewed from outside the wind tunnel through the telescope of a cathetometer. The combined methods enabled the contact position to be determined with an estimated accuracy of about 0.001 inch for measurements in the No. 1 wind tunnel. In the No. 2 wind tunnel, the optical method could not be used and only the electrical method was employed for the contact-position determination. Consequently, the estimated accuracy of this measurement in the No. 2 wind tunnel was of the order of 0.003 inch. Inasmuch as the contact position was used as the zero point of the bottom surface of the probe, the absolute position of the vertical scale is uncertain by this amount. At worst, such an uncertainty could mean a 20-percent error in θ_o, with a corresponding error of 2 percent in C_F. The effect of probe or model vibration on the measurement of pitot pressure is not known.

Computations necessary to obtain boundary-layer velocity profiles and other boundary-layer characteristics from the data obtained during surveys were carried out on a card-programmed electronic calculator with the usual assumptions of Prandtl number equal to unity and constant static pressure through the boundary layer. One difficulty ordinarily encountered with boundary-layer computations by these machines is that a long table search is required for obtaining Mach number from the ratio of static pressure (p) to pitot pressure (p_t'). This step was simplified

somewhat by employing 23 straight-line segments as an approximation to the curve of $(p_t'-p)/\frac{1}{2}\rho u^2$ as a function of p/p_t'. Coordinates of the end points of the straight-line segments are given in table II, which covers the range of Mach numbers from zero to infinity.

RESULTS OF MEASUREMENTS TESTING VALIDITY OF EXPERIMENTAL METHOD

Early in the course of measurements it became apparent that the uncorrected skin-friction data depended significantly on such things as the size and location of boundary-layer trip, the length of nose ahead of the cylindrical measuring section, and the particular wind tunnel in which the data were obtained. This situation arose primarily because the location of transition - and, hence, the effective origin of fully developed turbulence - varied with changes in each of these conditions. It was hoped that if the effective origin of turbulence were determined for each test condition, and if the production of completely turbulent flow by a boundary-layer trip were assured, then the final corrected data would not be sensitive to the techniques employed in obtaining them. Numerous supplementary tests, which are discussed below, were made in order to investigate such matters and thereby to determine the degree to which the final data depend on the particular experimental methods employed.

Tripping Devices to Insure Turbulent Flow

Surface-probe pitot-pressure surveys with various trips applied were made to find a satisfactory method of obtaining completely turbulent flow. Dimensions of the various trips investigated are given in figure 6. The results for $M_\infty = 2.9$ and for the lowest tunnel pressure employed in the No. 2 tunnel at this particular Mach number are shown in figure 7. The Mach number $(M)_{reference}$ used in the ordinate of this figure is the local value that would exist in inviscid flow, as determined by the method of characteristics. It may be seen that transition on the smooth body apparently occurred between about 4 and 7 inches from the cone tip. Consequently, some device, such as a boundary-layer trip, was needed to obtain a completely turbulent boundary layer over the cylinder. As figure 7 shows, trip 6 moved transition upstream some but not enough. Trip 5 appears sufficient, and trip 1, which is located the farthest upstream, appears more than sufficient under these particular conditions.

Although trip 5 was adequate at $M_\infty = 2.9$, it was not adequate at $M_\infty = 3.6$. Trip 1 proved to be adequate for every Mach number and Reynolds number investigated in the No. 2 wind tunnel; hence, it was selected for use in all final measurements of turbulent skin friction conducted in that particular tunnel. In the No. 1 wind tunnel, however, the turbulence level and Reynolds numbers obtainable are much lower, and it was found necessary to employ two trips in tandem (trips 2 and 4 proved adequate).

As an incidental note of possible interest, the point of beginning fuzziness in the boundary layer on various schlieren photographs (not shown) from the No. 2 tunnel was in all cases close to the apparent end of transition indicated by surface-pressure surveys. This correlation is believed not to be a general one, but dependent on the particular wind tunnel, since fair correlation was observed in the No. 1 tunnel with the apparent beginning of transition indicated by surface-pressure surveys.

An independent demonstration of the state of boundary-layer flow at the beginning station of measurement (station 0) was provided by the boundary-layer velocity-profile surveys. Typical examples from the No. 1 tunnel are shown in figure 8. With the addition of a trip, the actual velocity profiles (using y as ordinate, fig. 8(a)) were thicker than for the smooth body; whereas the dimensionless velocity profiles (using y/θ as ordinate, fig. 8(b)) were much fuller than corresponding profiles without a trip. The fuller profile in $(u/u_e, y/\theta)$ coordinates is more characteristic of turbulent profiles. Once the boundary layer was adequately tripped, further additions of tripping devices only increased the boundary-layer thickness, but did not alter its dimensionless velocity profile. Typical data from the No. 2 tunnel which demonstrate this latter point are shown in figure 9(a), and the results of measurements of skin-friction coefficient with various trips and without a trip are shown in figure 9(b). A curve is not faired through the transition-region data for the smooth cone-cylinder (circle points in figure 9(b)), inasmuch as these data are believed to exhibit primarily such things as the effects of turbulence level of the No. 2 tunnel. Also, the particular method employed to determine the effective boundary-layer origin is not applicable to transitional or laminar flow. It is apparent, though, that the differences in skin-friction coefficient between various trips are not large, and that the two data points for natural transition at the highest Reynolds numbers (near 20 million for $L/D = 13$) agreed well with the data obtained for tripped boundary layers.

A comparison of the velocity profile for the smooth body in the No. 1 tunnel (fig. 8(b)) with that for the same body in the No. 2 tunnel (fig. 9(a)) shows marked differences. In both cases the Reynolds number based on distance from cone tip to station 0 is about 2 million. Since transition on a smooth 10° cone at $M_\infty = 2$ begins at a Reynolds number of 3.1 million in the No. 1 tunnel, and at 0.7 million in the No. 2 tunnel (see ref. 52), it is to be expected that a laminar-type profile would be observed in the No. 1 tunnel and a transitional or near-turbulent-type profile would be observed in the No. 2 tunnel. Such expectations are borne out by the data of figures 8(b) and 9(a).

A point that should be noted from figure 8 is the appreciable difference sometimes obtained between velocity profiles at the top and bottom surfaces of the cylinder. This difference is due to a very small misalinement (a few tenths of a degree) of the model axis with the undisturbed stream direction. The high sensitivity of velocity profiles to small angles of attack on bodies of revolution has been noted before by several

investigators, and indicates that the circumferential variation in θ should be determined for such bodies when measuring skin friction by the momentum method. Such variations do not affect determinations of C_F by the direct-force method employed in this investigation because measurements of θ affect only the small correction to the force data. Moreover, such variations do not directly affect the skin-friction force measurements, since these were found to be independent of angle-of-attack variations up to the order of $\pm 1^\circ$.

Effect of Nose Shape

Two different nose shapes were employed at $M_\infty = 0.81$ to determine whether or not the subsonic data depended materially on this parameter. Although the measured momentum thickness at station 0 differed by a factor of approximately 2 for the two nose shapes shown in figure 10, the final skin-friction data were essentially independent of nose shape. (See fig. 10.) This should not be surprising in view of the fact that the only appreciable alterations in pressure distribution brought about by varying nose shape are confined to a small region downstream of station 0; hence, the main effect on average skin-friction coefficient is believed due to the differences in θ_0, which can be corrected for, just as for the case previously mentioned of different boundary-layer trips.

Attainment of Equilibrium in Blowdown Tunnel

Since tunnel No. 2 is of the blowdown type, the measurements in that tunnel were always made under conditions of slight heat transfer to the air stream. Figure 11(a) shows a typical time history of the wall temperature T_w expressed as a fraction of the reservoir total temperature T_t (which decreases at the rate of about 4° F per minute). Clearly, after about 5 minutes T_w/T_t became constant. The limiting value, 0.940 at $M_\infty = 3.4$, implies a recovery ratio $(T_w - T_\infty)/(T_t - T_\infty)$ of approximately 0.91 which is slightly higher than the usual recovery factor (0.89 ± 0.01) because of the small amount of heat transfer present even after T_w/T_t became constant. This small heat transfer (wall temperature within 2 percent of recovery temperature) is believed to have a negligible effect on skin friction. Only one set of measurements was made of C_F as a function of time, with the results shown in figure 11(b). The small variation probably is not significant, since 2-percent variation is within the limit of experimental error.

Comparison of Data From Wind Tunnels

At Mach numbers near 2.0, measurements could be made in tunnels No. 1 and No. 2 at overlapping Reynolds numbers. This provided an opportunity to compare data taken under considerably different conditions. As noted earlier, the No. 1 tunnel is a relatively low-turbulence-level tunnel (Re for transition on 10° cone is 3.1×10^6 at $M_\infty = 2.0$) of continuous-operation type in which the models were in thermal equilibrium. The No. 2 tunnel is a relatively high-turbulence-level tunnel (Re for transition on 10° cone is 0.7×10^6 at $M_\infty = 2.0$) of the blowdown type in which the models were releasing small amounts of heat to the stream, as discussed above. These combined differences, however, do not affect the observed velocity profiles at $M_\infty = 2$, as is evident from figure 12(a).[2] Likewise, these differences have no appreciable effect on the measured skin-friction coefficient at $M_\infty = 2$, as is evident from figure 12(b). It is not known whether the subsonic measurements, obtained only in the No. 2 tunnel, are affected by the relatively high turbulence level.

Effect of Pressure Gradient

At a Mach number of 2.0, the flexible-plate nozzle walls purposely were distorted in order to obtain friction data with various pressure distributions along the cylinder. Two such distributions, from a total of three, are shown in figure 13(a) plotted in the form of Mach number distribution. The corresponding skin-friction data are shown in figure 13(b). Evidently, the average turbulent skin-friction coefficient at this Mach number is not significantly affected by variations in pressure of the amounts investigated. It may be noted that the third distribution investigated (not shown) yielded the same skin friction to within about 2 percent as the two distributions shown. It is possible that the effect on local skin friction at individual points along the cylinder, which could not be measured, was considerably greater than the small integrated effect on average skin friction. It is also possible that the observed insensitivity to pressure gradient does not persist to Mach numbers far removed from 2.0 because the coefficient of the pressure-gradient term in the momentum equation for boundary layers happens to vanish for turbulent flow at Mach numbers of about 2.4 (see ref. 55 or 15).

Mention should be made of the fact that the two pressure distributions shown in figure 13(a) differ from each other by an amount greater than the difference between the normal pressure distributions of the

[2]Both velocity profiles shown in figure 12(a) were measured at the top surface of the survey model. In each of these cases, however, profiles obtained at the bottom surface agreed with those shown.

present investigation and a constant pressure. This difference in pressure distribution is comparable to the differences between pressure distributions for the various experiments on flat plates to which comparison with the present results will be made subsequently. Also, it is noted that the two pressure distributions shown differ from each other by roughly the same amount that the pressure distribution on a 3-percent-thick biconvex airfoil differs from a constant pressure; or, alternatively, by roughly the same amount that the pressure distribution on a parabolic-arc body of revolution of fineness ratio 15 differs from a constant pressure. The range of pressure variation covered by the present tests, therefore, is of some practical significance. Since no important effect on C_F of variations in pressure distribution was observed, the average skin-friction data to be presented later are considered applicable not only to the ideal case of constant pressure but also to thin pointed airfoils. Such data, though, apply only approximately to bodies of revolution not having a constant diameter since, in such cases, corrections should be made to allow for the relative thinning of the boundary layer over an expanding nose (Mangler type correction) and for the departure from two-dimensionality over an aftersection of the body due to the boundary-layer thickness becoming comparable to the body radius (L/D-type correction).

Although the departures from uniform pressure distribution did not affect average skin friction substantially, they did have noticeable effect on the velocity profiles over a small portion of the cylinder downstream of the cone-cylinder juncture. This is illustrated in figure 14 which shows five profiles at various stations along the cylinder. In the region near the shoulder (station 0) where the pressure varies most rapidly, the velocity profile is fuller than at downstream stations. This effect does not persist very far downstream, as may be seen from the figure. Little can be said about changes in dimensionless velocity profiles downstream of station 2 except that they were not greater than the random differences often observed between top and bottom surveys at a given station. Similarly, the rate of growth of boundary-layer thickness along the cylinder cannot be accurately specified because of this sensitive effect of model misalinement on the velocity profiles.

FINAL RESULTS AND DISCUSSION

Skin Friction for Various Values of L/D, M_∞, and Re

The principal results of the investigation showing C_F as a function of various parameters are presented in figures 15, 16, and 17. These figures will be discussed together in view of the interdependence of the various data. The fairing of curves in figure 15 has been influenced by the data of figure 16. In figure 16 the ratio C_F/C_{F_i} for a

given Reynolds number is plotted as a function of Re. The data shown are typical of all data obtained. In some cases, the data points indicate a small decrease in C_F/C_{F_i} with increasing Re (e.g., fig. 16(d)); in other cases, a small increase would be indicated (e.g., the data for $L/D = 13$ at $M_\infty = 2.5$ in fig. 15 would indicate such a trend if C_F/C_{F_i} were plotted as a function of Re); but in most cases, no systematic variation in C_F/C_{F_i} with Re is indicated. The variations sometimes observed are small enough to be within experimental error. Consequently, the curves in figure 15 have been faired to be consistent with the result of figure 16, indicating no substantial effect of Re on C_F/C_{F_i} over the Re range covered by a given model. If the Re range were increased many times, a small effect on C_F/C_{F_i} might be expected.

In figure 15, as well as in all other figures where it is not specified otherwise, the reference skin-friction coefficient C_{F_i} for zero Mach number arbitrarily is defined as the value given by the Kármán-Schoenherr equation for flat-plate flow $(C_{F_i})_{K\text{-}S}$. This arbitrary selection from the many semiempirical equations for C_{F_i} was made primarily because, at the Reynolds numbers for which measurements in compressible flow are available, it provides results intermediate to the results of other careful evaluations of incompressible turbulent skin friction. (See Appendix for comment on this point.) Discussion is presented later as to a more proper reference C_{F_i} for the present experiments on cylinders.

Plots of $C_F/(C_{F_i})_{K\text{-}S}$ as a function of M_∞ are presented in figure 17(a) and 17(b) for the three L/D values investigated. As noted in the figure subtitles, figure 17(a) presents individual data points for certain nominal Reynolds numbers; whereas figure 17(b) presents values picked from curves faired through measurements at all Reynolds numbers investigated. Both figures show no large effect of cylinder length on C_F. Since the maximum effect observed is only about twice the estimated experimental error, it is not considered significant that a few data points, especially in figure 17(a), appear inconsistent with the main body of data (fig. 17(b)) which exhibits the trend of increasing skin friction with increasing length-diameter ratio. The increment in C_F between $L/D = 8$ and $L/D = 23$ appears roughly constant for most Mach numbers, suggesting that perhaps at Mach numbers of the order of 5 or higher a substantial percentage effect of L/D on C_F might exist. This trend would be consistent with the increase in boundary-layer thickness at the higher Mach numbers, but it is by no means certain, in view of the fact that the differences observed are only about twice the estimated experimental error.

With regard to theoretical calculations of the effect of L/D on C_F, it is to be noted that the analyses of Jakob and Dow (ref. 49), Landweber (ref. 50), and Eckert (ref. 51) predict an increase in C_F with increasing L/D. The analysis of Jakob and Dow, which assumes that the rate of

boundary-layer growth along a cylinder is identical to that along a plate, predicts approximately 15-percent increase in friction for $L/D = 23$ as compared to $L/D = 8$. The analyses of Landweber and Eckert, which assumed that the relation between friction coefficient and boundary-layer thickness is identical for cylinder and plate, predict only 1.5-percent increase. The corresponding experimental result from the subsonic measurements is approximately a 4-percent increase. Unfortunately, the basic assumptions of these two analyses cannot be evaluated from the present experiments because of the previously mentioned difficulty of a circumferential variation of boundary-layer thickness often encountered at a fixed longitudinal station.

Thus far, the reference value employed for C_{F_i} of cylinders is the Kármán-Schoenherr value for flat-plate flow. It is now apparent that the correct reference value for C_{F_i} will depend somewhat on the L/D ratio of the cylinder. Consequently, the true effect of M_∞ on C_F for a given L/D would have to be evaluated by using values of C_{F_i} appropriate for each value of L/D. Sufficient subsonic measurements were made to provide such an evaluation. An experimental value $(C_{F_i})_{exp}$ of skin-friction coefficient for each cylinder at $M_\infty = 0$ was determined from the two sets of subsonic measurements by applying a correction to allow for the small effect of compressibility at subsonic Mach numbers. The correction was determined by averaging the predicted values of C_F/C_{F_i} given by the equations of Cope, Tucker II, and Wilson, and amounted to a 2.5- and 6.1-percent increase in the data for $M_\infty = 0.51$ and $M_\infty = 0.81$, respectively. The two values so obtained were averaged for each cylinder. Values of $(C_{F_i})_{exp}$ deduced in this manner from the data of figure 17(a) for L/D ratios of 8, 13, and 23 are 2.5, 0.2, and -0.6 percent lower, respectively, than the value predicted by the Kármán-Schoenherr equation. The corresponding corrections from the data of figure 17(b) are 2.2, 0.2, and -1.4 percent, respectively. With $(C_{F_i})_{exp}$ so determined, plots of $C_F/(C_{F_i})_{exp}$ were made. Results from the data of figure 17(b) are shown in figure 17(c). There is little scatter in this latter plot (mean deviation from faired curves is about 1 percent) and no clearly discernible effect of L/D. Consequently, data points for the various fineness ratios were averaged at each Mach number. The resulting values, tabulated in tables III(a) and III(b), corresponding, respectively, to data of figures 17(a) and 17(b), can be compared directly with flat-plate data, in view of the absence of any appreciable L/D effect on $C_F/(C_{F_i})_{exp}$. The values in table III(b) are perhaps more representative of the main body of experimental data than the values in table III(a), although the differences are not significant. Table III(a) was published previously in reference 36.

Comparison of Results With Other Investigations

In figure 18 two velocity profiles from the present investigation on cylinders are compared with a velocity profile from Coles' measurements (ref. 15) on a flat plate. These profiles are for $M_\infty = 2.0$ and for Reynolds numbers near 6 million. It is seen that there is an appreciable difference between the profiles for plate and cylinder, the cylinder profile being the fuller of the two.

A compilation of results from the several experiments in which skin friction was determined by direct-force measurements is presented in figure 19.[3] Here, again, the ratio of compressible to incompressible skin friction is plotted as a function of Mach number. The Reynolds numbers of the three experiments are sufficiently comparable, in view of the results shown in figure 16, so that the indicated effect of Mach number is not obscured by such differences in Reynolds number. As noted in figure 19, the Kármán-Schoenherr c_{f_i} has been used as reference for the data of Coles and Hakkinen;[4] whereas experimental values of incompressible friction have been used as reference for the present data. Because of the use of a different reference c_{f_i} and a different effective Reynolds number (see Appendix), the data points representing Coles' experiments in figure 19 are appreciably, though perhaps not significantly, different from points that would be obtained by plotting values tabulated

---

[3]The direct-force measurements of Bradfield, DeCoursin, and Blumer (ref. 41) on cones are not included in this figure. It is noted, however, that these data for cones indicate higher friction than the data in figure 19. The direct-force data of Liepmann and Dhawan (ref. 38) and Weiler and Hartwig (ref. 43), for which the effective origin of turbulence was not determined, also are not shown in figure 19.

In an earlier paper (ref. 36) Coles' uncorrected data of reference 39 were used for comparison, inasmuch as his corrected data were not available at the time of that writing. In figure 19 Coles' data have been referred to an average effective Reynolds number for reasons explained in the Appendix.

[4]Although Hakkinen made subsonic measurements of local friction, he did not determine the effective Reynolds number for these low-speed data. His effective Re for the supersonic data is based on distance from the position of maximum shear, which he determined.

The value of c_{f_i} corresponding to the Kármán-Schoenherr equation is

$$c_{f_i} = \frac{0.557\, C_{F_i}}{0.557 + 2\sqrt{C_{F_i}}}$$

where C_{F_i} is as defined previously.

in reference 15. Consequently, without some comment the apparently excellent agreement of Coles' c_f data with the present C_F data might be misleading. For example, Coles' data points would be lowered about 2 percent if the so-called Prandtl-Schlichting equation for c_{f_i} were used, but would be raised about 3 percent if the equation proposed by Coles for c_{f_i} were used. Similarly, his data points would be either raised or lowered the order of 4 percent, depending on the values of effective Reynolds number assigned to his data. Thus, the unusually close agreement indicated in figure 19 can be taken as meaning for certain only the order of ±5-percent agreement between c_f/c_{f_i} and C_F/C_{F_i}, although the true agreement may possibly be as close as the figure suggests.

Beyond a Mach number of about 5, the absence of experimental data renders the estimation of skin friction increasingly uncertain as the Mach number is progressively increased. Perhaps a measure of the minimum uncertainty involved would be that indicated by the difference between the estimates made by Cope and Tucker. Although it is not shown in figure 19, these two estimates do not differ greatly from the experiments below $M_\infty = 5$. They diverge considerably from each other above $M_\infty = 5$, as illustrated in the figure. Cope and Tucker each have advanced two estimates; the particular curves shown in figure 19 represent Cope's "log-law" analysis and Tucker's "mean-reference-temperature" hypothesis, both of which have been recomputed for the common basis of a recovery factor of 1, a 0.76-power variation of viscosity with temperature, and the Kármán-Schoenherr equation for incompressible flow. It may be noted that several other analyses (e.g., Wilson and Frankl-Voishel) also agree fairly well with the skin-friction measurements below $M_\infty = 5$, and that many other equations easily could be constructed which would do likewise. Consequently, without experimental confirmation of the basic assumptions involved, the agreement in end result of any one of the various analyses with experiment does not necessarily represent any more than would be represented by agreement of an empirical equation with experiment.

In figure 20 a comparison is made between the mean curve from the direct-force data of figure 19 and numerous other measurements (the effective Reynolds numbers for which are listed in table V) wherein the average skin friction was determined indirectly from boundary-layer surveys using the conventional momentum method.[5] The agreement is not good. Except for the present measurements, these various momentum-method data have all been referred to the Kármán-Schoenherr equation

[5]Experiments wherein the virtual origin of turbulence, and, hence, the effective-length Reynolds number, was not determined experimentally are excluded from figure 20. Measurements in this category are, for example, the tunnel-wall measurements of Cope (ref. 42) and Weiler and Hartwig (ref. 43). Also, the preliminary measurements of Bloom (ref. 47) have been excluded because of possible condensation effects in his experiments.

for C_{F_i}. Excluding one point, the many momentum-method determinations indicate higher friction than the direct-force data. This particular point, from the present experiments at $M_\infty = 3.6$, represents a single determination in the blowdown (No. 2) tunnel at a single Reynolds number. The accuracy of this point is not known. In contrast, the point from the present experiments plotted at $M_\infty = 2.0$ represents the average of many determinations on two different models in the continuous-operation (No. 1) tunnel at various Reynolds numbers between 3 million and 10 million, all determinations of which showed from 5- to 10-percent-higher friction than the direct-force data. For these measurements on cylinders, an average of the surveys on top and bottom of the cylinder was employed in all cases, with the friction force deduced from the difference in surveys at stations 0 and 7. Similar surveys at intermediate stations were employed to evaluate the small correction for pressure gradient in the momentum integral equation.

There are at least two additional reasons for possible errors in the conventional momentum method of determining skin friction, even for flows wherein the pressure is constant and transverse secondary flow does not exist. First, the reading of a pitot tube near the surface where the greatest momentum decrement occurs is not entirely certain because of probe interference and perhaps vibration; second, the conventional momentum method neglects the contribution of the Reynolds normal stress to the momentum integral. Estimates of this latter contribution made by Ross (ref. 56), for the case $M_\infty = 0$, indicate that the conventional momentum method would yield values about 2 percent too high. It is noted that the correction factor of Ross involves principally the shape parameter (ratio of displacement to momentum thickness) which greatly increases as the Mach number increases.

It should be noted that a given error in evaluating the effective Reynolds number for momentum-method C_F data results in much greater final error than for direct-force c_f data. This situation arises because Re enters directly into the ordinate for momentum-method determinations of average friction ($C_F = 2R_\theta/Re$); whereas it enters only indirectly as the less sensitive abscissa for direct-force determinations of local friction. For example, a 10-percent error in Re easily may exist for most measurements presented in figure 20, and this would bring about an 8-percent error in a momentum-method determination of C_F/C_{F_i}; whereas it would bring about only 2-percent error in a direct-force determination of c_f/c_{f_i}.

Direct-force measurements of skin friction, on the other hand, may be slightly in error if a small floating element is employed because of the "gap effect" which at present has not been precisely evaluated. This effect is indicated by the available data (refs. 15, 38, and 48) to be only a few percent. The present measurements on cylinders are believed to be free of any such effect. Consequently, it appears that the

conventional momentum method is not reliable for accurate determinations of friction. The exact reasons for this unreliability have yet to be established.

CONCLUDING REMARKS

From a practical viewpoint the principal results of the present research can be summarized concisely: (1) The skin-friction coefficient for cylinders in axial flow is not greatly affected by variations in cylinder length-diameter ratio; (2) the ratio of compressible to incompressible friction is essentially independent of Reynolds number over the range of present experiments; and (3) measurements of average skin friction by the conventional momentum method for the case of zero heat transfer and zero pressure gradient do not agree well with direct-force measurements.

Although considerable attention has been paid (especially in the Appendix) to small differences that probably are of more interest to research workers than to practical engineers, sight should not be lost of the fact that agreement between the various direct-force measurements is quite satisfactory, particularly as regards the effect of Mach number on skin friction. The small uncertainties arising in the comparison of direct-force skin-friction measurements from several sources have stemmed primarily from the difficulties always involved in accurately determining an effective-length Reynolds number and in accurately knowing the proper reference values for incompressible flow. It is believed that both difficulties mentioned have been met satisfactorily in the present experiments on cylinders: the first, by the laborious technique of making boundary-layer surveys at upstream stations; and the second, by making measurements at subsonic speeds on the same apparatus as was used for supersonic speeds.

Apart from the above observations concerning detailed results of the investigation, there are several remarks that should be made here regarding application of the results. It might appear that the difficulty of determining an effective-length Reynolds number could be avoided by employing momentum-thickness Reynolds number (Re_θ) as the reference parameter. In this regard, however, caution should be exercised because of the doubt cast on the accuracy of the conventional momentum method by the data comparison of figure 20. Uncertainties in the measured momentum decrement can arise because of probe interference, particularly near the wall, and because of the neglect of Reynolds normal stresses in the often-used relations between measured momentum thickness and skin friction.

Primarily because of custom, the effect of Mach number on skin friction has been presented for the particular conditions of constant-length Reynolds number wherein free-stream viscosity is employed as reference

viscosity. Comparison with zero-heat-transfer flight data should be viewed in this light because the ratio of wall to free-stream viscosity is greatly different between wind tunnel and flight, and because experience to date has indicated the wall viscosity of a turbulent boundary layer to be much more significant than the free-stream viscosity. It is possible that in the prediction of flight characteristics a more proper yet equally convenient reference viscosity for wind-tunnel measurements would be the wall viscosity multiplied by the ratio - that would exist in flight - of free-stream to wall viscosity. On this basis, the expected effect of Mach number in reducing friction coefficients for flight conditions of zero heat transfer would be essentially the same up to Mach numbers near 2, as is indicated by figure 19 of this report, but would be about a 7-percent-greater reduction at a Mach number of 4, and even greater reductions at higher Mach numbers. Because of this effect, and the effect that might be expected due to significant differences in the ratio of specific heats between flight and wind-tunnel-temperature conditions, the direct application of wind-tunnel results to flight conditions, even for the special case considered of zero heat transfer, should be viewed with reservation at Mach numbers near or above about 4. Future research could be directed profitably toward finding methods by which wind-tunnel measurements of boundary layers at such Mach numbers can be utilized with confidence to predict flight characteristics.

Ames Aeronautical Laboratory
National Advisory Committee for Aeronautics
Moffett Field, Calif., Dec. 9, 1953

APPENDIX

NOTES ON DIFFICULTIES INVOLVED IN COMPARING AND ANALYZING VARIOUS MEASUREMENTS OF SKIN FRICTION

There are two fundamental difficulties always involved in analyzing various high-speed measurements of skin friction (and, presumably, heat transfer). The first concerns the reliable determination of an effective Reynolds number for completely turbulent flow; such determination is necessary for meaningful data since the location of transition differs greatly between various wind tunnels as well as between wind-tunnel and flight conditions. The second difficulty concerns the proper reference values for friction in an incompressible flow; such uncertainty is becoming conspicuous because the differences in proposed formulas for friction at low speeds are greater than the accuracy or scatter of either Coles' measurements or the present measurements. Accordingly, some discussion of these troublesome items is in order.

A good illustration of both difficulties may be obtained, for example, by attempting to compare the effect of Reynolds number on the ratio of compressible to incompressible friction as determined from the present measurements and from Coles' measurements. The maximum range of Re obtainable in the present tests represents a variation of about 4:1, over which no systematic variation of C_F/C_{F_i} with Re could be detected. The measurements of Coles represent a variation in Re of about 15:1, though at somewhat lower Reynolds numbers. The combined sets of data for $M_\infty = 2.50$, as shown in figure 21(a),[6] cover a variation in Re of about 50:1. Over this range Coles' data appear to indicate a small decrease in the ratio of compressible to incompressible friction as Re is increased. As is evident from figure 21(b), however, this small variation is less than the certainty with which the true reference values for c_{f_i} are now known, since the use of a different reference c_{f_i}, such as that proposed by Schultz-Grunow (ref. 7), Schlichting (ref. 57), or Coles (ref. 15), yields results appreciably different from results based on the Kármán-Schoenherr equation. It is difficult to determine which reference c_{f_i} is most appropriate to use. From the fundamental concepts involved, the soundest equation is the one used by Coles, which might be called the "complete" Kármán equation inasmuch as it was first developed by Kármán (ref. 13) but differs from the simplified form usually associated with his name. This complete equation is based solely on the two empirical velocity-profile similarity laws referred to in the Introduction. The

[6] Coles' data are plotted 1.3 percent higher than the corresponding tabulated values of reference 15 in order to convert his data, which were taken at $M_\infty = 2.57$, to the common value 2.50 used in this figure. Similarly, corrections of less than 1 percent have been applied to the present data to convert them to $M_\infty = 2.50$.

difficulty with this equation concerns the method of evaluating the four constants which appear in it. Coles made an elaborate evaluation of these constants from velocity-profile measurements only. Before Coles' evaluation was available, the writers determined the same four constants from profile measurements of Schultz-Grunow (ref. 7) and Klebanoff-Diehl (ref. 58), obtaining significantly different values. It would appear better to use shear measurements together with velocity-profile measurements in evaluating such constants. This apparently has not yet been done. As a result, the equation proposed by Coles does not agree as well with the available direct-force measurements of c_{f_i} as does, for example, the equation of Kármán-Schoenherr. (A plot of the Kármán-Schoenherr equation for c_{f_i} on figure 1 of Coles' thesis will verify this.) On the other hand, the present measurements of average friction on cylinders extrapolated to two-dimensional flow (L/D = 0) yield values perhaps a little closer to Coles' C_{F_i} than to the Kármán-Schoenherr C_{F_i}. Also, the recent C_{F_i} measurements of Hughes (ref. 3) are closer to Coles' evaluation of C_{F_i} than to the Kármán-Schoenherr equation. All such differences are only the order of ±5 percent from a mean, but this is considerably greater than the apparent error of Coles' measurements. It is believed that a definitive evaluation of c_{f_i} and C_{F_i} for flat plates has yet to be made.

Although the uncertainty of about ±5 percent in the proper reference c_{f_i} for flat-plate data presumably could be removed by some definitive measurements of skin friction in low-speed flow, a second obstacle remains to a clear-cut comparison with Coles' data that may not be removed by future measurements: The effective Reynolds number determination for Coles' data is less certain than the apparent accuracy of his measurements would warrant. The method Coles used in determining the abscissa of the data of figure 21(a) was to employ the observed position of maximum shear stress, which is located near the end of the transition region, as the virtual origin of turbulence. Inasmuch as the data points not only are remarkably consistent, but represent three plate locations, two types of transition, and many tunnel pressures, considerable credence must be attached to this method of determining an effective-length Reynolds number. However, a second method employed (and preferred) by Coles to determine the virtual origin yielded substantially different results, corresponding to about 6-percent-greater skin friction at $M_\infty = 2.57$, and less at higher Mach numbers. This latter method involved relating the $c_f(R_\theta)$ curves of compressible and incompressible flow in a manner (details are given in Coles' thesis) such that an effective-length Reynolds number could be deduced. A third method, not employed by Coles, would be to utilize the measured shear on the upstream floating element of his plate at a given tunnel pressure to calculate the virtual origin, and then to apply this to determine the value of Re to be assigned to shear measurements on downstream elements at the same pressure. In this latter method an assumption, such as the independence of c_f/c_{f_i} as

function of Reynolds number, would be required. Data points of Coles for which all three of the above-mentioned methods can be applied are presented in table IV. The average of the three determinations of effective Reynolds number given in the last column has been employed for comparisons with Coles' data (except in fig. 21) since, in the opinion of the present writers, there is no decisive choice among the three methods. It is unfortunate that boundary-layer surveys were not made at upstream stations along Coles' plate, for such surveys would make comparison with the present data and other data more certain.

REFERENCES

1. Schoenherr, Karl E.: Resistance of Flat Surfaces Moving Through a Fluid. Soc. Nav. Arch. and Marine Eng. Trans., vol. 40, 1932, pp. 279-313.

2. Locke, F. W. S., Jr.: Recommended Definition of Turbulent Friction in Incompressible Fluids. Bur. Aero., Navy Dept., (Design) Res. Div., DR Rep. 1415, 1952.

3. Hughes, G.: Frictional Resistance of Smooth Plane Surfaces in Turbulent Flow - New Data and Survey of Existing Data. Trans. Inst. Nav. Arch., vol. 94, 1952, pp. 287-322

4. Liepmann, Hans Wolfgang, and Laufer, John: Investigations of Free Turbulent Mixing. NACA TN 1257, 1947.

5. Townsend, A. A.: The Structure of the Turbulent Boundary Layer. Proc. Camb. Phil. Soc., vol. 47, pt. 2, April 1951, pp. 375-395.

6. Gurjienko, G. A.: Universal Logarithmic Law of Velocity Distribution as Applied to the Investigation of Boundary Layer and Drag of Streamline Bodies at Large Reynolds Numbers. NACA TM 842, 1937, (From Rep. No. 257 of the Central Aero-Hydrodynamical Institute, Moscow, 1936)

7. Schultz-Grunow, F.: New Frictional Resistance Law for Smooth Plates. NACA TM 986, 1941. (From Luftfahrtforschung, vol. 17, no. 8, Aug. 1940, pp. 239-46)

8. Klebanoff, P. S.: Characteristics of Turbulence in a Boundary Layer With Zero Pressure Gradient. NBS Rep. 2454, 1953.

9. von Kármán, Th.: On Laminar and Turbulent Friction. NACA TM 1092, 1946. (From Zeitschrift für angewandte Mathematik und Mechanik, vol. 1, no. 4, Aug. 1921, pp. 233-252.)

10. Darcy, H.: Recherches experimentales relatives aux mouvement de l'eau dans les tuyaux. Memoires des Savants Etrangers, vol. 15, 1858, pp. 141, 265.

11. Stanton, T. E.: The Mechanical Viscosity of Fluids. Proc. Roy. Soc. London, Series A, vol. 85, 1911, p. 366. (See also Stanton, T. E. and Pannel, J. R.: Similarity of Motion in Relation to the Surface Friction of Fluids. Phil. Trans. Roy. Soc., Series A, vol. 214, 1914, p. 199.)

12. Fritsch, W.: Einfluss der Wandrauhigkeit auf die Turbulente Geschwindigkeitsverteilung in Rinnen. Z.f.a.M.M., vol. 8, 1928, p. 199.

13. von Kármán, Th.: Theorie des Reibungswiederstandes. From Hydromechanische Probleme des Schiffsantriebs. G. Kempf and E. Foerster (Hamburg), 1932.

14. Millikan, C. B.: A Critical Discussion of Turbulent Flows in Channels and Circular Tubes. Proc. V. Int. Cong. Appl. Mech., Cambridge, Mass., 1938, pp. 386-392.

15. Coles, D.: Measurements in the Boundary Layer on a Smooth Flat Plate in Supersonic Flow. PhD Thesis, C.I.T., 1953.

16. von Kármán, Th.: The Problems of Resistance in Compressible Fluids, Reale Accademia D'Italia, Rome, 1936.

17. Frankl, F. J, and Voishel, V.: Turbulent Friction in the Boundary Layer of a Flat Plate in a Two-Dimensional Compressible Flow at High Speeds. NACA TM 1053, 1943. (From Central Aero-Hydrodynamical Inst., Moscow, 1937, Rep. No. 321)

18. Cope, W. F.: The Turbulent Boundary Layer in Compressible Flow. NPL Eng. Dept., British ARC 7634, Nov. 1943. (See also Cope, W. F.: Notes and Graphs for Boundary Layer Calculations in Compressible Flow. British ARC Current Papers No. 89, 1952.)

19. Clemmow, D. M.: The Turbulent Boundary Layer Flow of a Compressible Fluid Along a Flat Plate. British Director of Guided Weapons Res. and Development, DGWRD 50/6, Aug. 1950.

20. Eckert, Hans Ulrich: Characteristics of the Turbulent Boundary Layer on a Flat Plate in Compressible Flow from Measurements of Friction in Pipes. Jour. Aero. Sci., vol. 17, no. 9, Sept. 1950, pp. 573-584.

21. Wilson, Robert E.: Turbulent Boundary-Layer Characteristics at Supersonic Speeds - Theory and Experiment. Jour. Aero. Sci., vol. 17, no. 9, Sept. 1950, pp. 585-594.

22. Van Driest, E. R.: Turbulent Boundary Layer in Compressible Fluids. Jour. Aero. Sci., vol. 18, no. 3, Mar. 1951, pp. 145-160, 216.

23. Monaghan, R. J.: Comparison Between Experimental Measurements and a Suggested Formula for the Variation of Turbulent Skin Friction in Compressible Flow. British ARC C.P. No. 45 (13260), 1951.

24. Smith, F., and Harrop, R.: The Turbulent Boundary Layer with Heat Transfer and Compressible Flow. TN No. Aero. 1759, British R.A.E., Feb. 1946.

25. Rubesin, Morris W., Maydew, Randall C., and Varga, Steven A.: An Analytical and Experimental Investigation of the Skin Friction of the Turbulent Boundary Layer on a Flat Plate at Supersonic Speeds. NACA TN 2305, 1951.

26. Tucker, Maurice: Approximate Turbulent Boundary-Layer Development in Plane Compressible Flow Along Thermally Insulated Surfaces With Application to Supersonic-Tunnel Contour Correction. NACA TN 2045, 1950.

27. Tucker, Maurice: Approximate Calculation of Turbulent Boundary-Layer Development in Compressible Flow. NACA TN 2337, 1951.

28. Li, Ting-Yi, and Nagamatsu, Henry T.: Effects of Density Fluctuations on the Turbulent Skin Friction of an Insulated Flat Plate at High Supersonic Speeds. GALCIT Memo No. 5, May 1951.

29. Proceedings of the Bureau of Ordnance Symposium on Aeroballistics. Nov. 16-17, 1950. Comments by E. R. Van Driest on paper by R. E. Wilson. NAVORD Rep. 1651, pp. 264-267.

30. Ferrari, Carlo: Study of the Boundary Layer at Supersonic Speeds in Turbulent Flow: Case of Flow Along a Flat Plate. Quart. Appl. Math., vol. 8, no. 1, April 1950, pp. 33-57.

31. Young, George B. W., and Janssen, Earl: The Compressible Boundary Layer. Jour. Aero. Sci., vol. 19, no. 4, April 1952, pp. 229-236, 288.

32. Dorodnitsyn, A. A.: Boundary Layer in Compressible Gas. Prikladnaia Matematika i Mekhanika, vol. VI, no. 6, 1942, pp. 449-486

33. Kalikhman, L. E.: Heat Transmission in the Boundary Layer. NACA TM 1229, 1949. (From Prikladnaia Matematika i Mekhanika, vol. 10, no. 4, 1946, pp. 449-474)

34. Tetervin, Neal: Approximate Formulas for the Computation of Turbulent Boundary-Layer Momentum Thicknesses in Compressible Flows. NACA WR L-119. (ACR No. L6A22, March 1946)

35. Donaldson, C. duPont: On the Form of the Turbulent Skin-Friction Law and its Extension to Compressible Flows. NACA TN 2692, 1952.

36. Chapman, D. R. and Kester, R. H.: Measurements of Turbulent Skin Friction on Cylinders in Axial Flow at Subsonic and Supersonic Velocities. Jour. Aero. Sci., vol. 20, no. 7, July 1953, pp. 441-448.

37. Rubesin, M. W.: A Modified Reynolds Analogy for the Compressible Turbulent Boundary Layer on a Flat Plate. NACA TN 2917, 1953.

38. Liepmann, H. W., and Dhawan, Satish: Direct Measurements of Local Skin Friction in Low-Speed and High-Speed Flow. Proc. of First U. S. Nat. Cong. App. Mech., June 11-16, 1951, Chicago, 1952. (See also Dhawan, Satish: Direct Measurements of Skin Friction. NACA TN 2567, 1952.)

39. Coles, Donald: Direct Measurement of Supersonic Skin Friction. Jour. Aero. Sci., vol. 19, no. 10, Oct. 1952, p. 717.

40. Brinich, Paul F., and Diaconis, Nick S.: Boundary-Layer Development and Skin Friction at Mach Number 3.05. NACA TN 2742, 1952.

41. Bradfield, W. S., DeCoursin, D. G., and Blumer, C. B.: Characteristics of Laminar and Turbulent Boundary Layer at Supersonic Velocity. Univ. of Minn., Inst. of Tech. Res., Rep. 83, 1952.

42. Cope, W. F.: The Measurement of Skin Friction in a Turbulent Boundary Layer at a Mach Number of 2.5, Including the Effect of a Shock Wave. Proc. Roy. Soc., Ser. A, vol. 215, no. 1120, Nov. 1952.

43. Weiler, J. E., and Hartwig, W. H.: The Direct Determination of Local Skin Friction Coefficient. Univ. of Texas Def. Res. Lab., CF 1747, (UT/DRL 295), Jan., 1952.

44. Spivack, H. M.: Experiments in the Turbulent Boundary Layer of a Supersonic Flow. North American Aviation, Inc., Rep. No. CM-615 (AL-1052), 1950.

45. Monaghan, R. J. and Johnson, J. E.: The Measurement of Heat Transfer and Skin Friction at Supersonic Speeds. Part II. Boundary Layer Measurements on a Flat Plate at M = 2.5 and Zero Heat Transfer. British ARC. CP 64, (13,064), 1952.

46. Ladenburg, I. R. and Bershader, Daniel: Optical Studies of Boundary Layer Phenomena on a Flat Plate at Mach Number 2.35. Princeton Univ., Dept. of Phys., Dec. 1952.

47. Bloom, H. L.: Preliminary Survey of Boundary-Layer Development at a Nominal Mach Number of 5.5. NACA RM E52D03, 1952.

48. Hakkinen, Raimo J.: Measurements of Skin Friction in Turbulent Boundary Layers at Transonic Speeds. PhD. Thesis, C.I.T., 1953.

49. Jakob, Max, and Dow, W. M.: Heat Transfer from a Cylindrical Surface to Air in Parallel Flow With and Without Unheated Starting Sections. A.S.M.E. Transactions, vol. 68, no. 2, Feb. 1946, pp. 123-134.

50. Landweber, L.: Effect of Transverse Curvature on Frictional Resistance. DTMB Rep. 689, March 1949.

51. Eckert, H. U.: Simplified Treatment of the Turbulent Boundary Layer Along a Cylinder in Compressible Flow. Jour. Aero. Sci., vol. 19, no. 1, Jan. 1952, pp. 23-28.

52. Stine, Howard A., and Scherrer, Richard: Experimental Investigation of the Turbulent-Boundary-Layer Temperature-Recovery Factor on Bodies of Revolution at Mach Numbers from 2.0 to 3.8. NACA TN 2664, 1952.

53. Bradfield, W. S. and Yale, G. E.: Small Pitot Tubes with Fast Pressure Response Time. Jour. Aero. Sci., vol 18, no. 10, Oct. 1951, pp. 697-698.

54. Patterson, John L.: A Miniature Electrical Pressure Gage Utilizing a Stretched Flat Diaphram. NACA TN 2659, 1952.

55. Eckert, Hans U.: Approximate Method for Compressible Turbulent Boundary Layers with Pressure Gradient. WADC Tech. Note WCRR 53-3 (RDO No. 467-3-15), Jan. 1953.

56. Ross, Donald: Evaluation of the Momentum Integral Equation for Turbulent Boundary Layers. Jour. Aero. Sci., vol. 20, no. 7, July 1953, p. 502.

57. Schlichting, H.: Grenzschient-Theorie. Verlag Und Druck G. Braun (Karlsruhe, Germany), 1951.

58. Klebanoff, P. S. and Diehl, Z. W.: Some Features of Artificially Thickened Fully Developed Turbulent Boundary Layers With Zero Pressure Gradient. NACA TN 2475, 1951.

TABLE I.- LOCATION OF SURVEY STATIONS

Survey station	Distance from cone apex, in.
0	3.11
1	3.48
2	3.96
3	4.82
4	6.07
5	8.09
6	9.93
7	14.90

NACA

TABLE II.- TWENTY-FOUR POINT APPROXIMATION TO PITOT-PRESSURE EQUATION

$\frac{p}{p_t'}$	$\frac{p_t'-p}{\frac{1}{2}\rho u^2}$	$\frac{p}{p_t'}$	$\frac{p_t'-p}{\frac{1}{2}\rho u^2}$	$\frac{p}{p_t'}$	$\frac{p_t'-p}{\frac{1}{2}\rho u^2}$
1.0000	1.0000	0.7000	1.1412	0.4000	1.4131
.9600	1.0146	.6700	1.1606	.3500	1.4696
.9100	1.0344	.6400	1.1818	.2500	1.5791
.8700	1.0515	.6100	1.2040	.1900	1.6438
.8300	1.0700	.5800	1.2285	.1200	1.7174
.7900	1.0901	.5500	1.2546	.0900	1.7485
.7600	1.1060	.5200	1.2831	.0600	1.7791
.7300	1.1230	.4900	1.3143	0	1.8400

NACA

TABLE III.- VALUES OF $C_F/(C_{F_i})_{exp}$ FROM EXPERIMENTS ON CYLINDERS (INDEPENDENT OF L/D FOR RANGE INVESTIGATED)

(a) From data of figure 17(a)

M	$C_F/(C_{F_i})_{exp}$
0.51	0.985
.81	.929
1.99	.745
2.49	.671
2.95	.623
3.36	.578
3.60	.551

(b) From data of figure 17(b)

M	$C_F/(C_{F_i})_{exp}$
0.51	0.994
.81	.924
1.99	.757
2.49	.672
2.95	.630
3.36	.571
3.60	.552

NACA

TABLE IV.- EFFECTIVE REYNOLDS NUMBER (IN MILLIONS) FOR EXPERIMENTS OF COLES

M_∞	c_f	R_θ	Uncorrected $U_e x/\nu_e$	Corrected (a)			Average Re
				Re_1	Re_2	Re_3	
2.57	0.00181	6,600	4.84	4.2	[b]6.1	4.4	(c)
2.58	.00166	10,200	8.32	7.7	10.3	7.8	8.6
3.70	.00162	4,100	3.54	[b]2.6	4.0	(d)	(c)
3.70	.00138	7,560	7.25	6.4	8.6	7.6	7.5
4.51	.00148	3,470	3.52	[b]1.8	3.6	(d)	(c)
4.55	.00122	6,590	6.83	5.6	8.2	6.0	6.6
4.50	.00155	2,900	3.37	(e)	2.8	(d)	(c)
4.54	.00126	5,240	6.91	(e)	6.2	6.1	(c)

[a] Re_1 determined from position of maximum shear (interpolated from ref. 15)
Re_2 determined from R_θ and $c_{f_i}(R_{\theta_i})$ relationship (ref. 15)
Re_3 determined from shear on upstream element, assuming c_f/c_{f_i} independent of Reynolds number

[b] Correction exceeds 25 percent of $U_e x/\nu_e$

[c] Average of three values not possible or considered unreliable because of large magnitude of correction

[d] Flow not fully turbulent over upstream element at this pressure

[e] Re_1 not determined by Coles

NACA

TABLE V.- VALUES OF Re FOR DATA OF FIGURE 20

Experiment	$Re \times 10^{-6}$	Method of determining Re
Wilson	10	extrapolate θ to zero
Spivack	12.5	extrapolate θ to zero
Rubesin-Maydew-Varga	7	ratio c_f/C_F taken as average of various theoretical predictions
Monaghan-Johnson	3	extrapolate θ to zero
Brinich-Diaconis	3 to 18	extrapolate θ to zero
Ladenburg-Bershader	2.7	distance from end of transition as indicated by schlieren
Coles	8.6 at $M_\infty = 2.58$ 7.5 at $M_\infty = 3.70$ 6.6 at $M_\infty = 4.55$	average of three methods, see table IV
Chapman-Kester	10 at $M_\infty = 3.8$, 3 to 10 at $M_\infty = 2.0$	extrapolate θ to zero

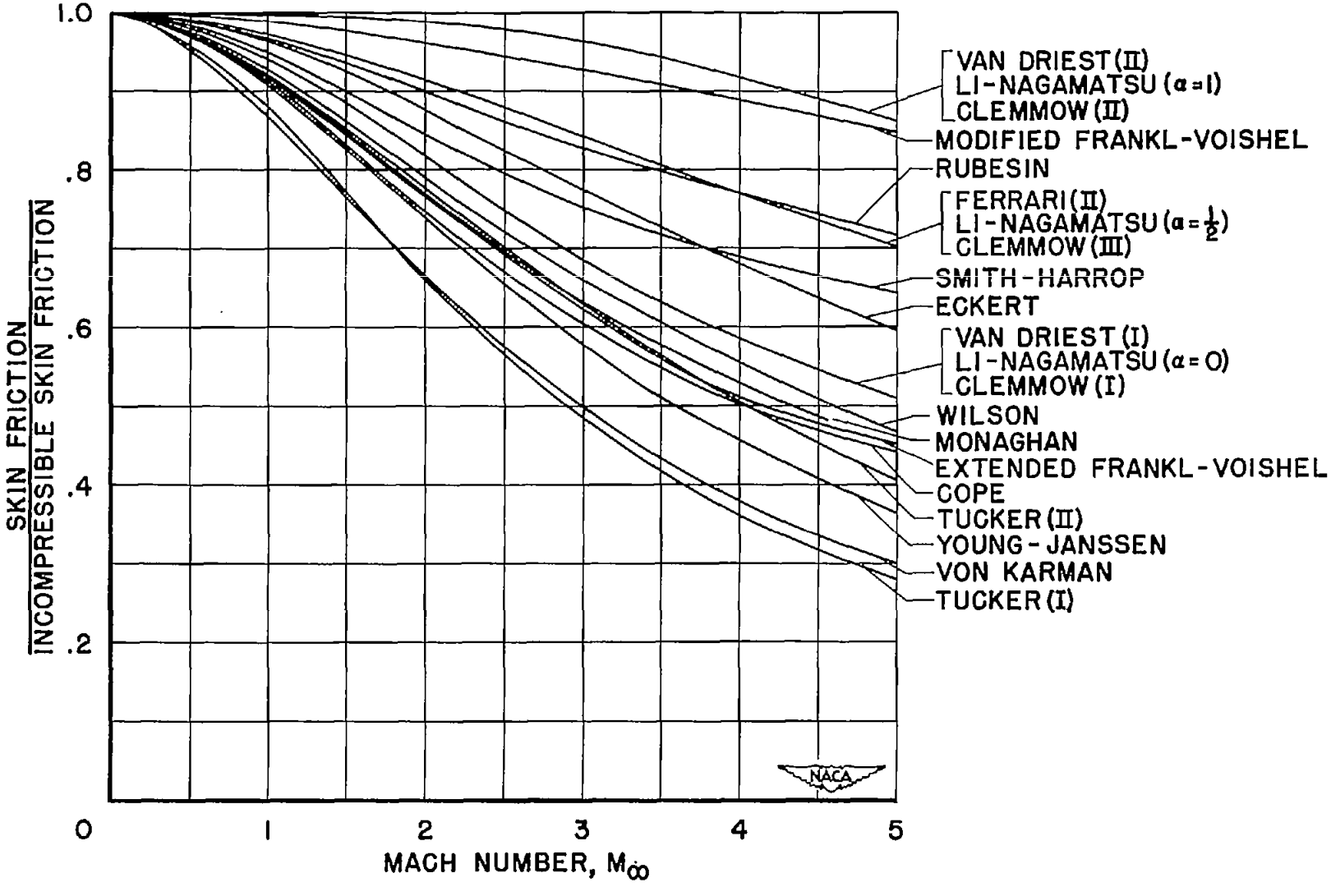

Figure 1.- Results of various analyses of turbulent skin friction for compressible flow over an insulated flat plate.

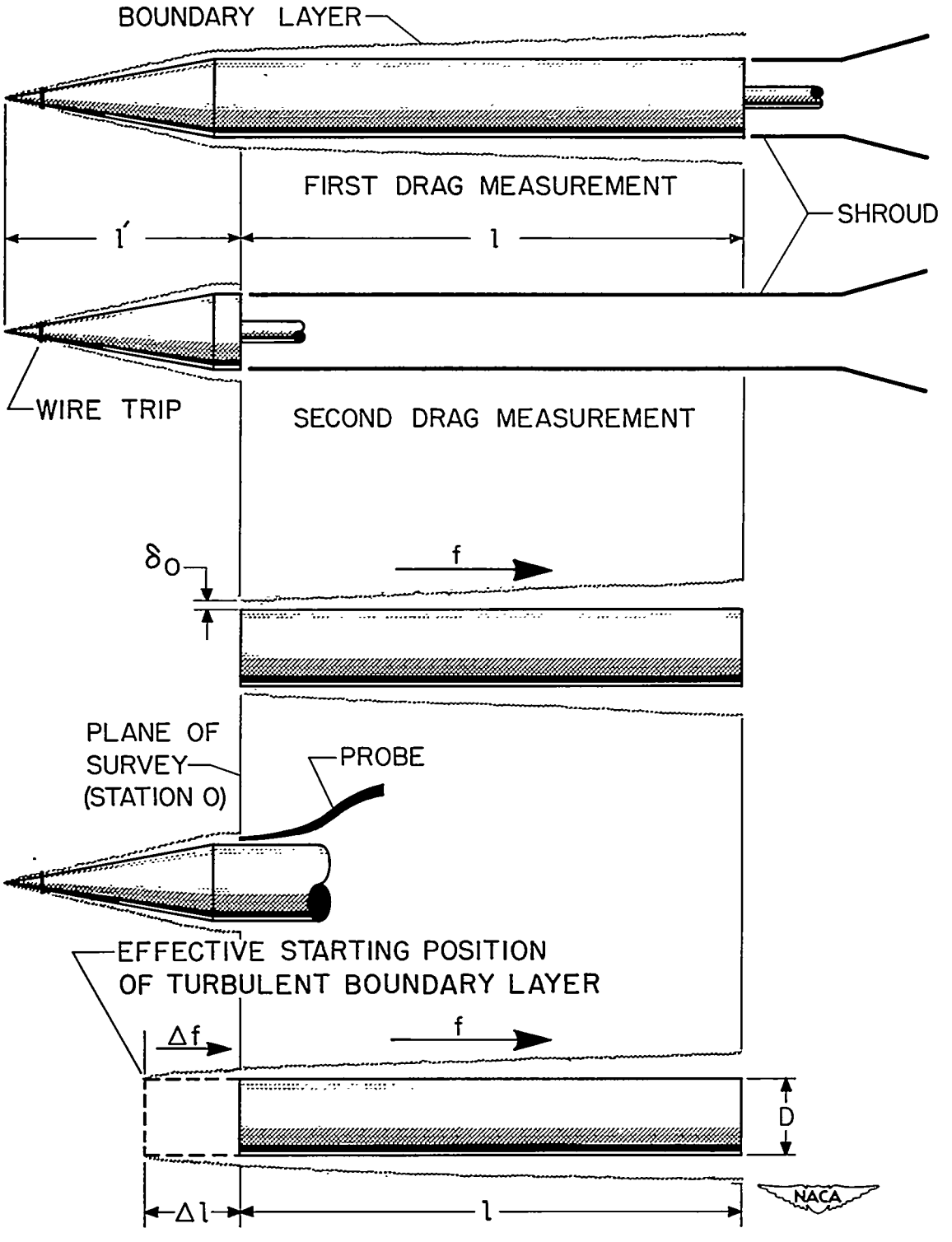

Figure 2.- Sketch illustrating method of determining friction force and effective starting position of turbulent boundary layer.

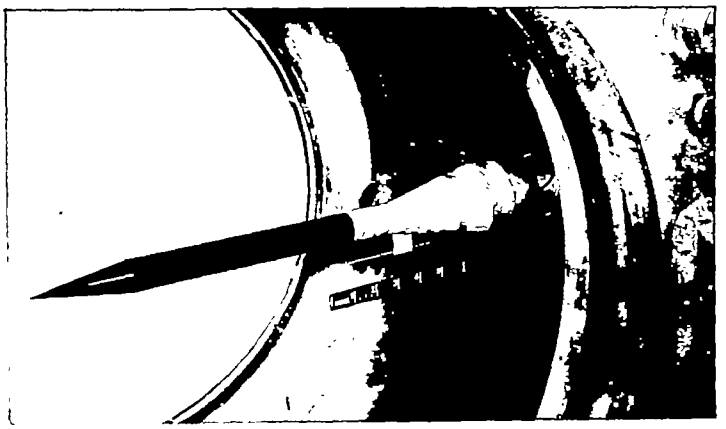

A-15964

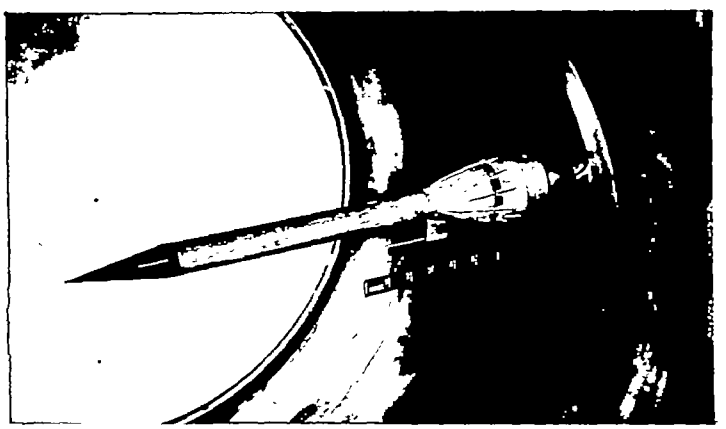

A-15965

Figure 3.- Cone-cylinder models mounted in wind tunnel.

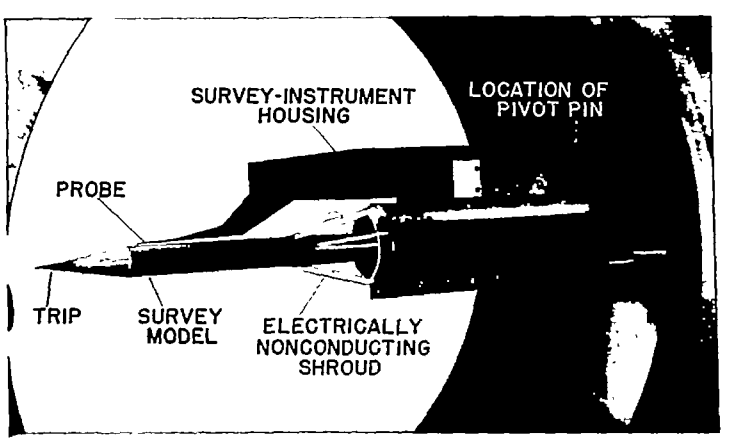

A-17040.1

Figure 4.- Apparatus used for survey across boundary layers.

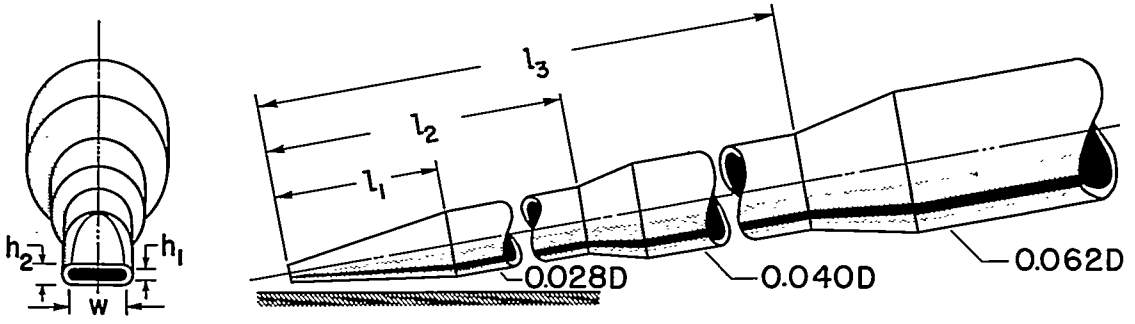

PROBE NO.	DIMENSIONS IN INCHES						USED IN TUNNEL	USED FOR DATA OF FIGURES
	h_1	h_2	w	l_1	l_2	l_3		
1	0.001	0.003	0.016	0.10	0.21	0.97	NO. 1	8, 12a, 18
2	.004	.011	.020	.18	.36	.97	NO. 2	9a, 12a, 14

NACA

Figure 5.- Probes employed for boundary-layer surveys.

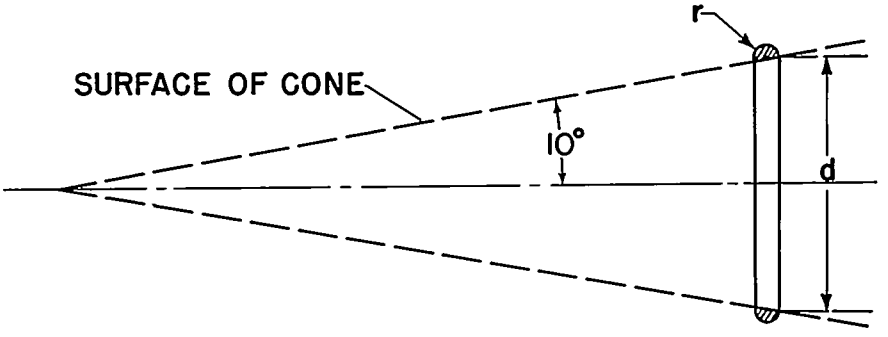

TRIP NO.	d	r
1	0.187 IN.	0.010 IN.
2	.187	.005
3	.250	.010
4	.250	.005
5	.500	.010
6	.750	.010

NACA

Figure 6.- Dimensions of boundary-layer trips.

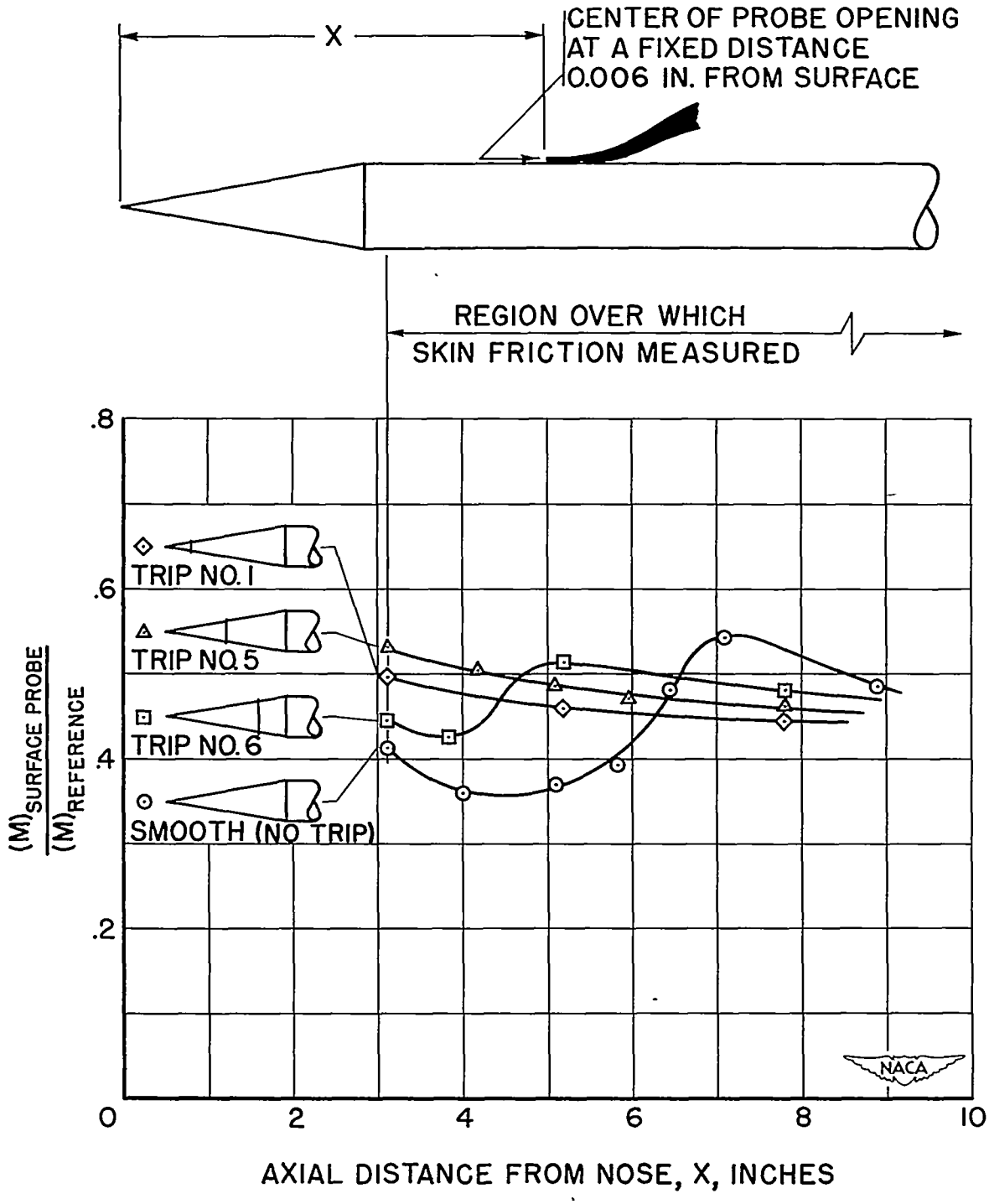

Figure 7.- Effect of various trips on transition as determined by near-surface pitot-pressure measurements; M_∞=2.9, Re=0.5x10^6 per inch; tunnel No. 2.

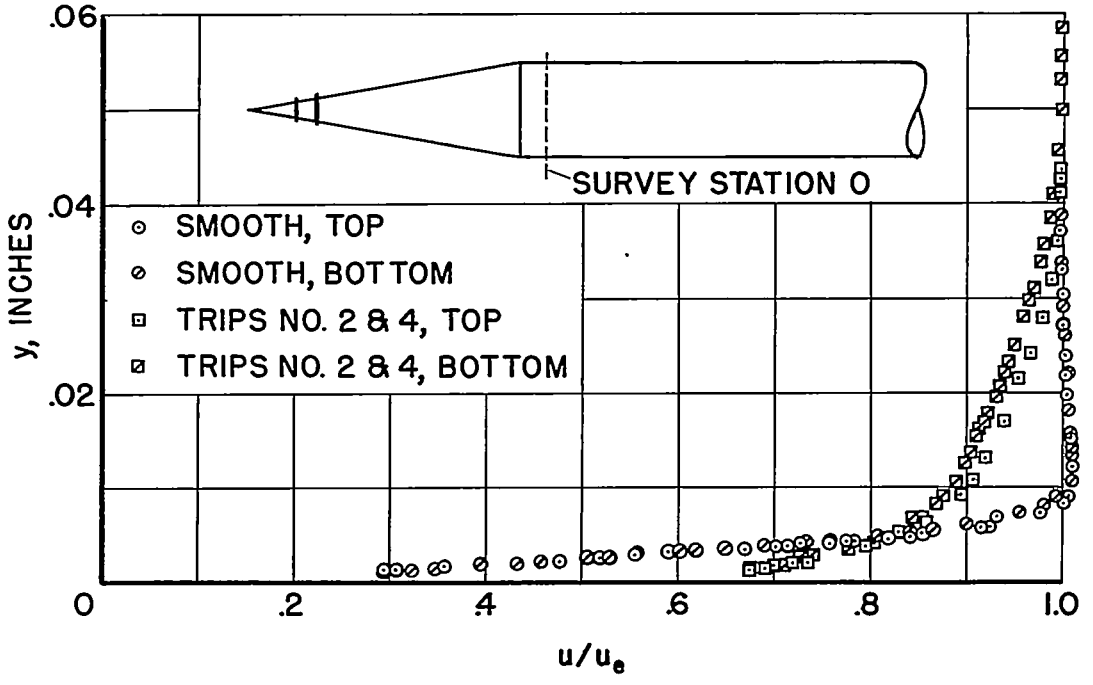

(a) Dimensional profiles.

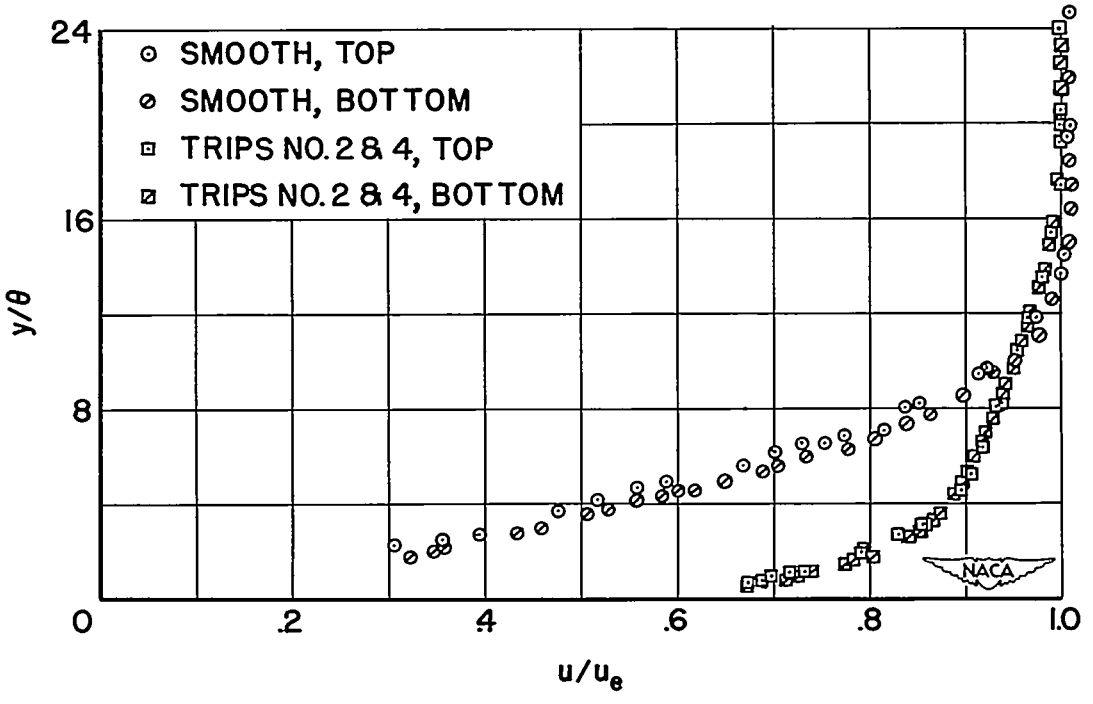

(b) Dimensionless profiles.

Figure 8.- Effect of trip on velocity profile at station 0 (beginning of cylindrical surface over which skin friction was measured); M_∞=2.0, Re=0.64x10^6 per inch; tunnel No. 1.

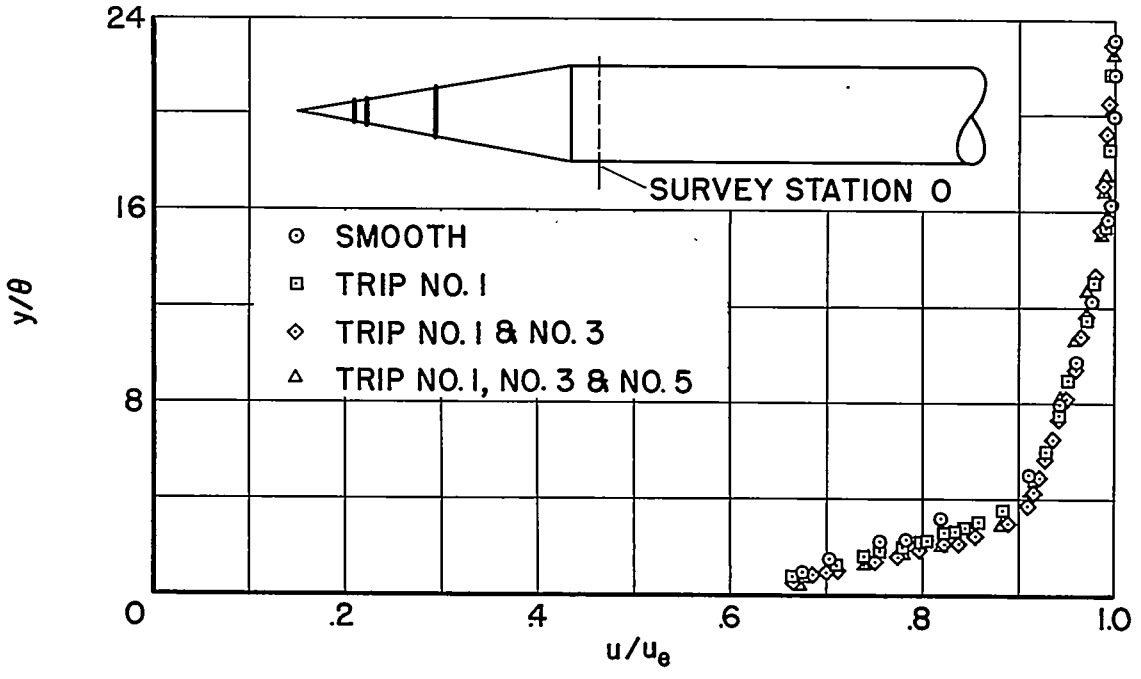

(a) Effect on velocity profile; Re=0.66x10^6 per inch.

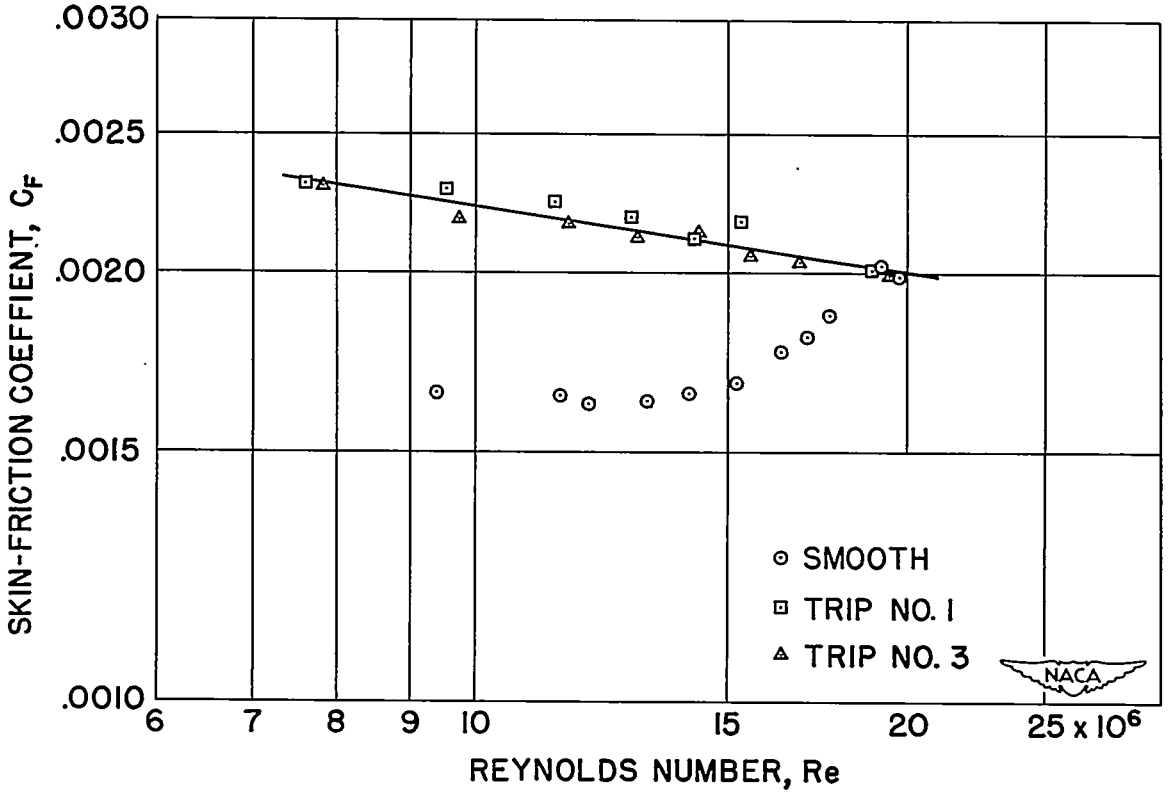

(b) Effect on skin friction; L/D = 13.

Figure 9.- Measurements with various trips alone and in combination; M_∞=2.0; tunnel No. 2.

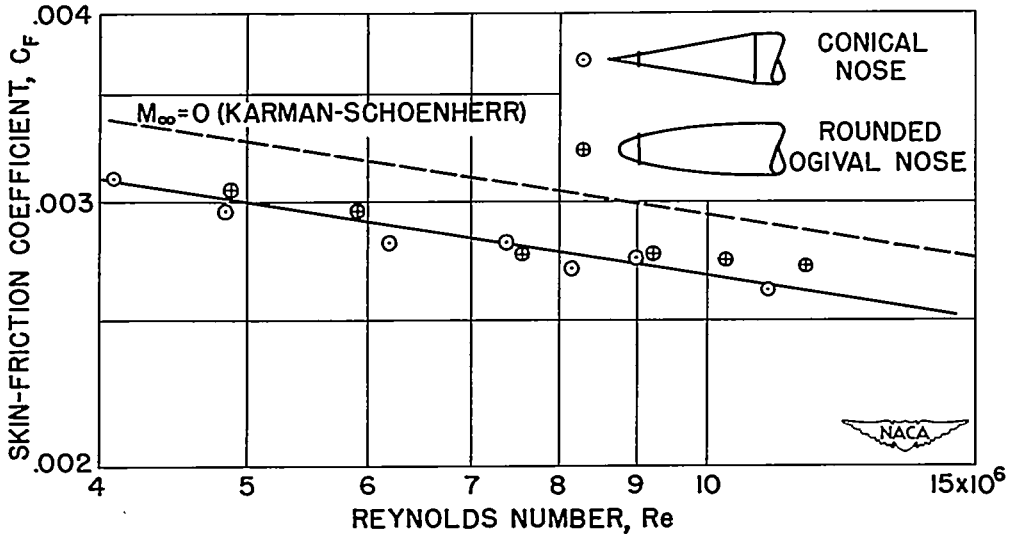

Figure 10.- Measurements of skin friction at subsonic velocity using different nose shapes; M_∞=0.81, L/D = 8.

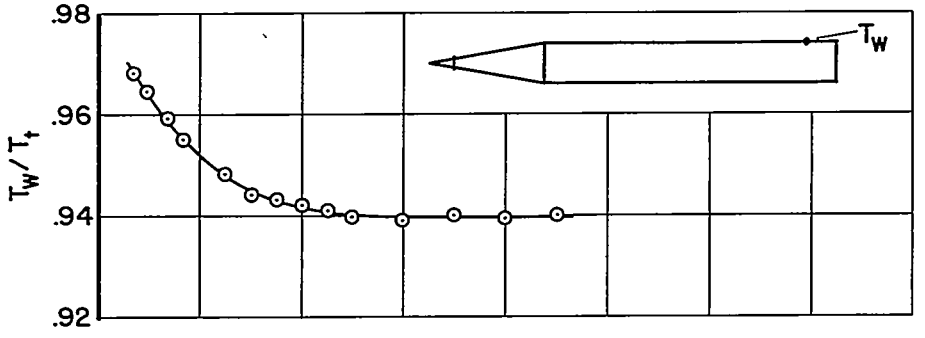

(a) Surface temperature; M_∞=3.4, Re=7.2x10^6.

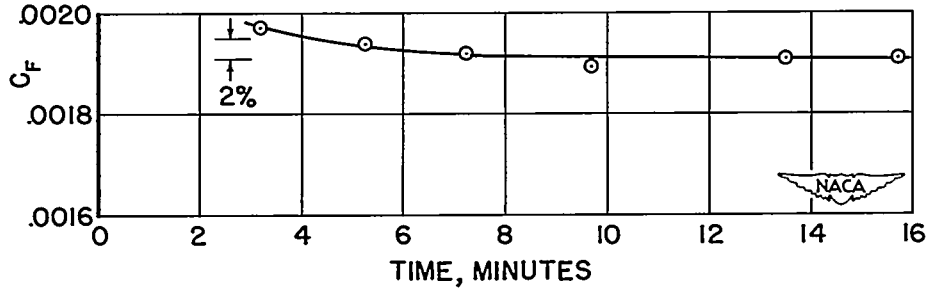

(b) Skin friction; M_∞=2.95, Re=9.5x10^6, L/D = 13.

Figure 11.- Attainment of near-equilibrium conditions in tunnel No. 2.

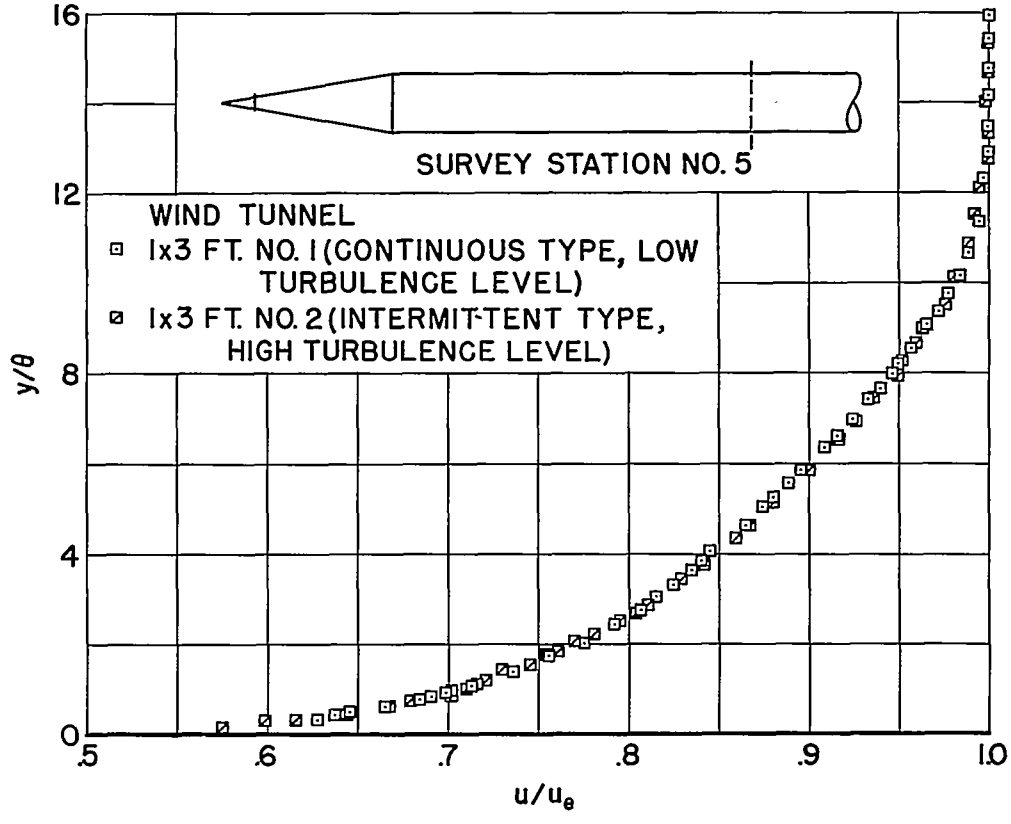

(a) Comparison of velocity profiles; Re=0.66x10^6 per inch.

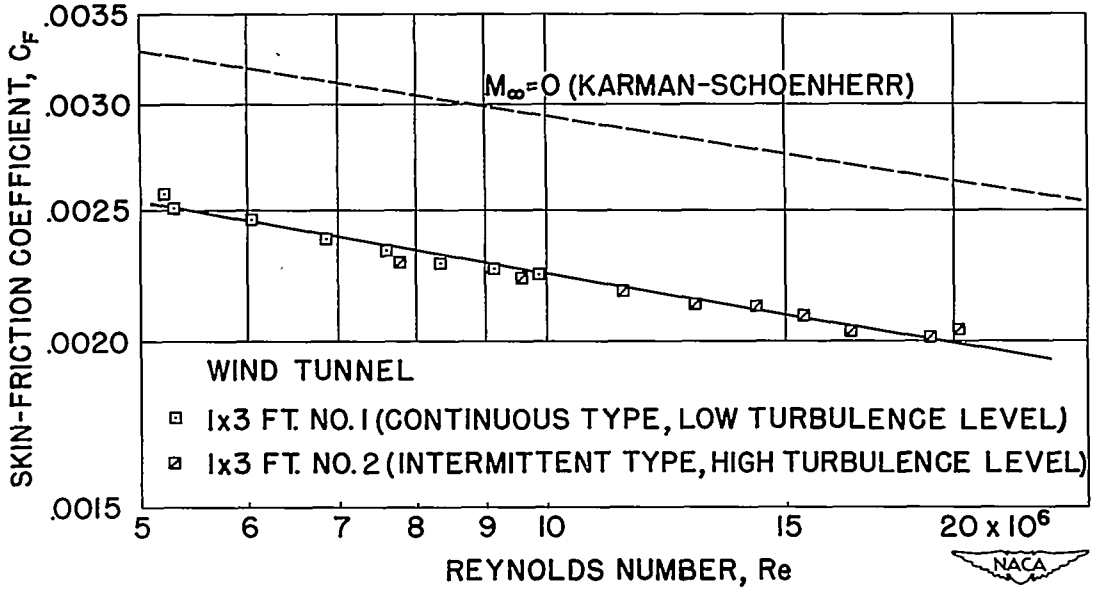

(b) Comparison of skin friction; L/D = 13.

Figure 12.- Comparison of measurements in the two wind tunnels employed; M_∞=1.98.

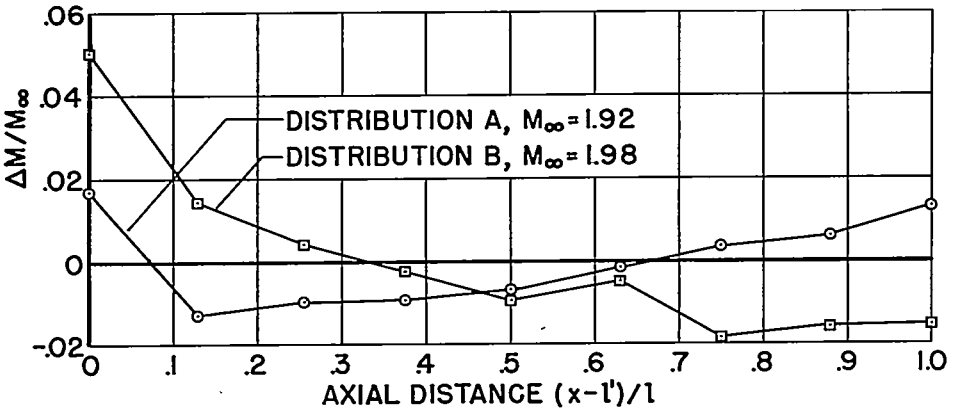

(a) Mach number distribution.

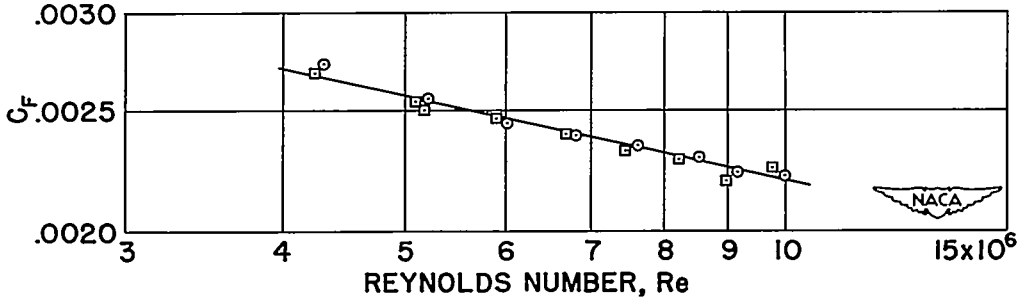

(b) Skin friction for distributions A and B.

Figure 13.- Absence of significant effect of a moderate variation in pressure distribution on average skin-friction coefficient; L/D = 13; tunnel No. 1.

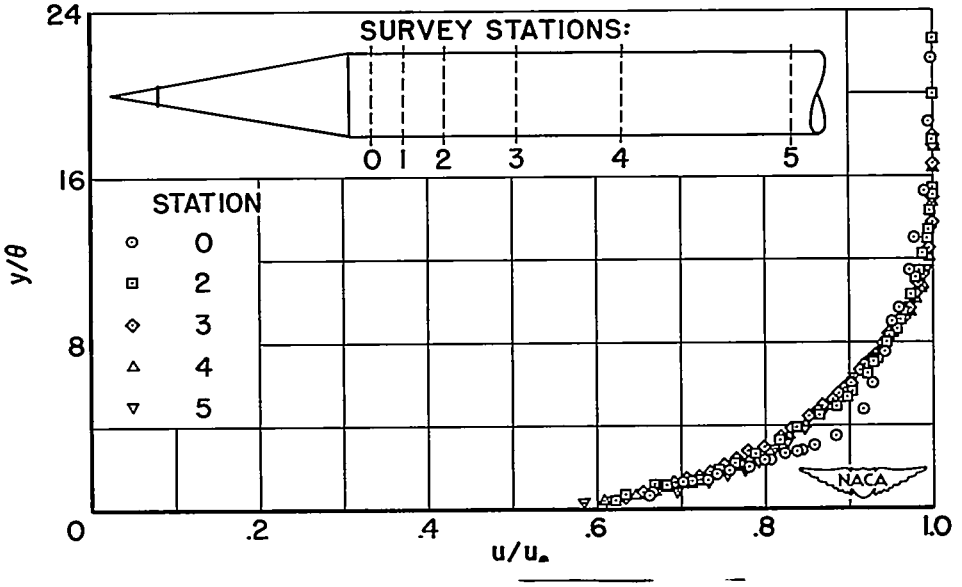

Figure 14.- Development of boundary-layer profile along cylindrical surface; M_∞=2.0, Re=0.66x10^6 per inch; tunnel No. 2.

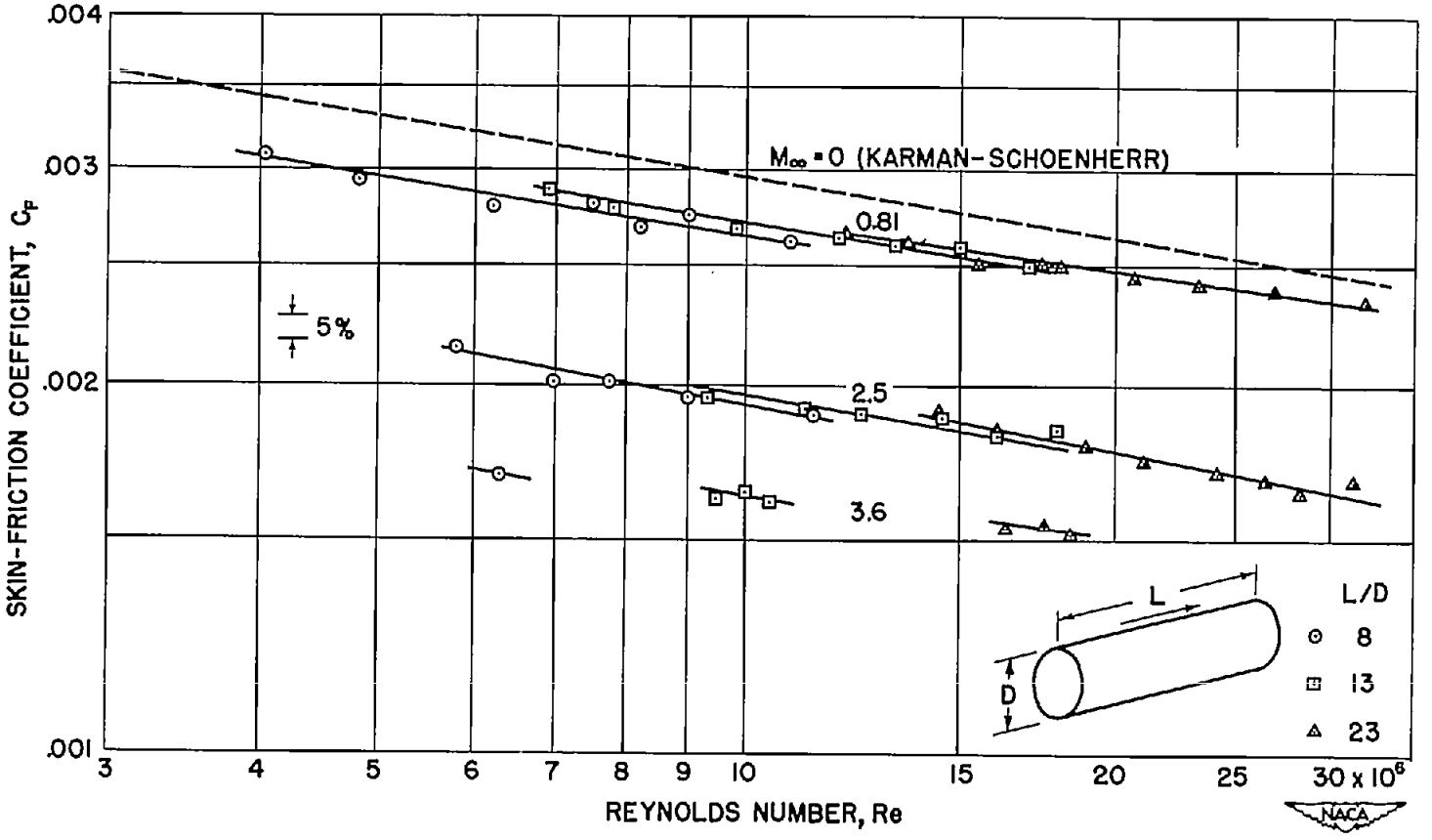

Figure 15.- Effect of Reynolds number, Mach number, and length-diameter ratio on skin friction; tunnel No. 2.

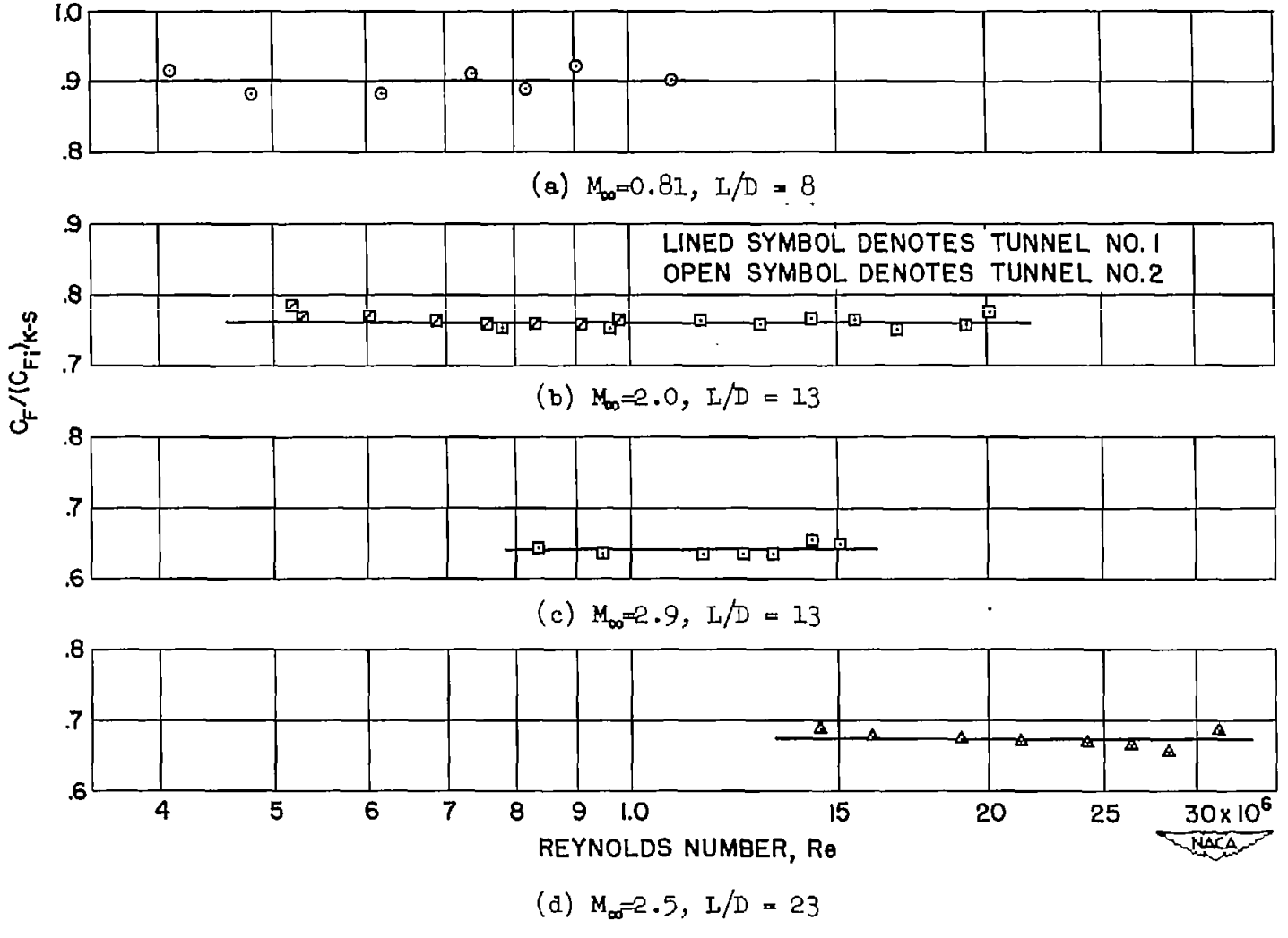

Figure 16.- Absence of significant effect of Reynolds number on $C_F/(C_{F_i})_{K-S}$ for moderate range of Reynolds number.

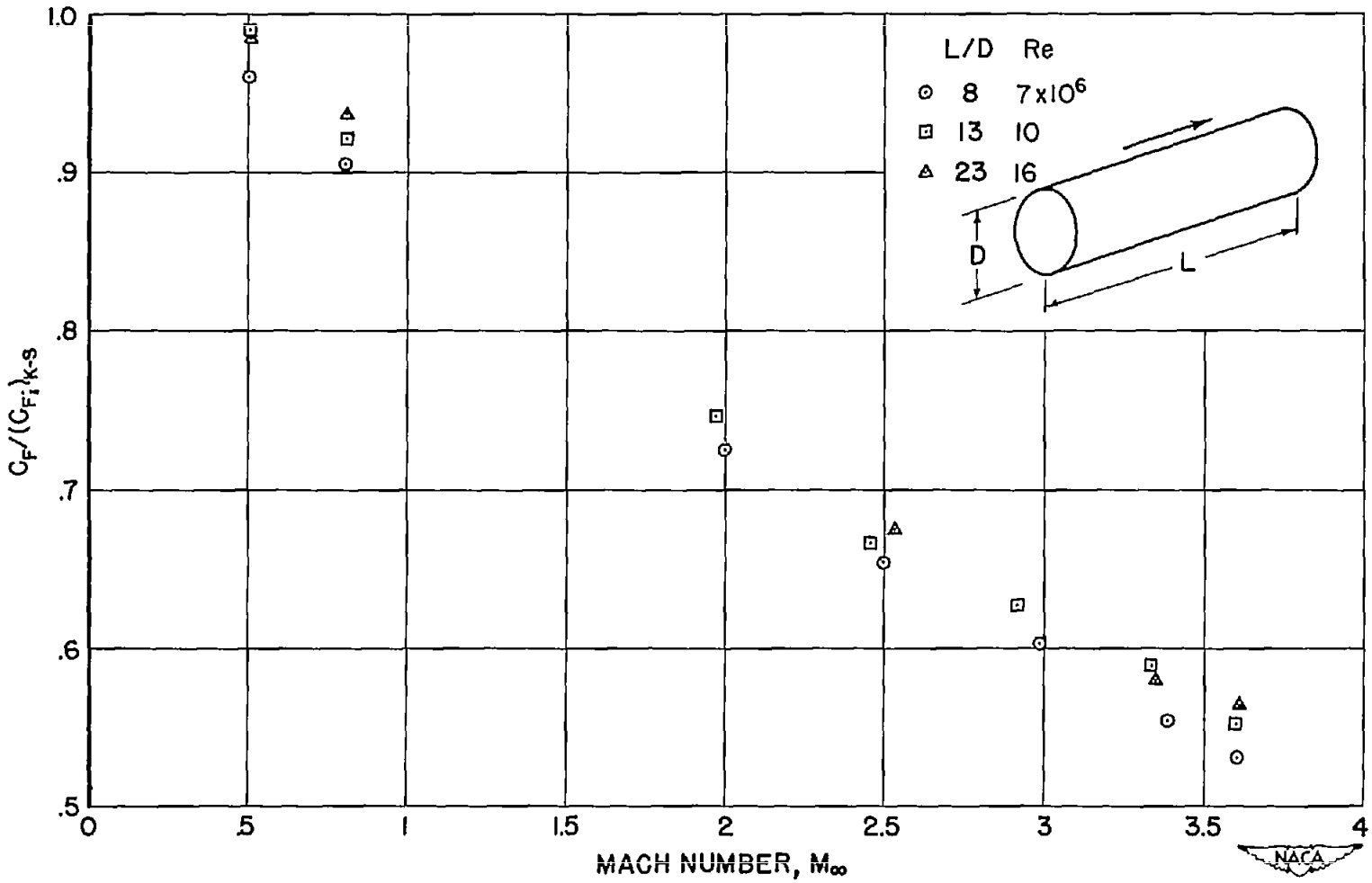

(a) Referred to Kármán-Schoenherr C_{F_i}. (Plotted points represent individual measurements at Re nearest designated value.)

Figure 17.- Effect of Mach number on skin friction; tunnel No. 2.

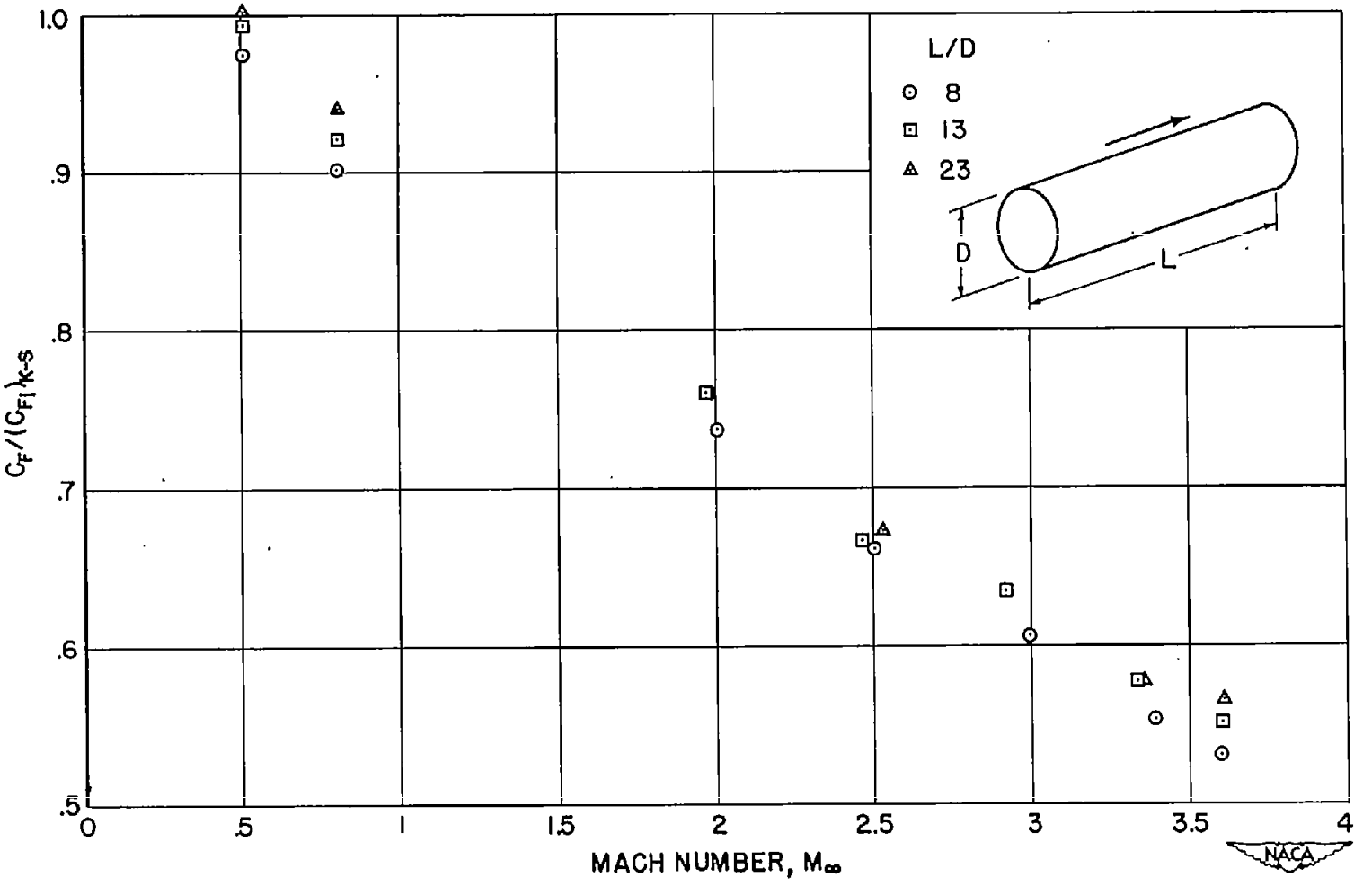

(b) Referred to Kármán-Schoenherr C_{F_1}. (Plotted points represent values from curves faired through all measurements for a fixed M_∞ and L/D.)

Figure 17.- Continued.

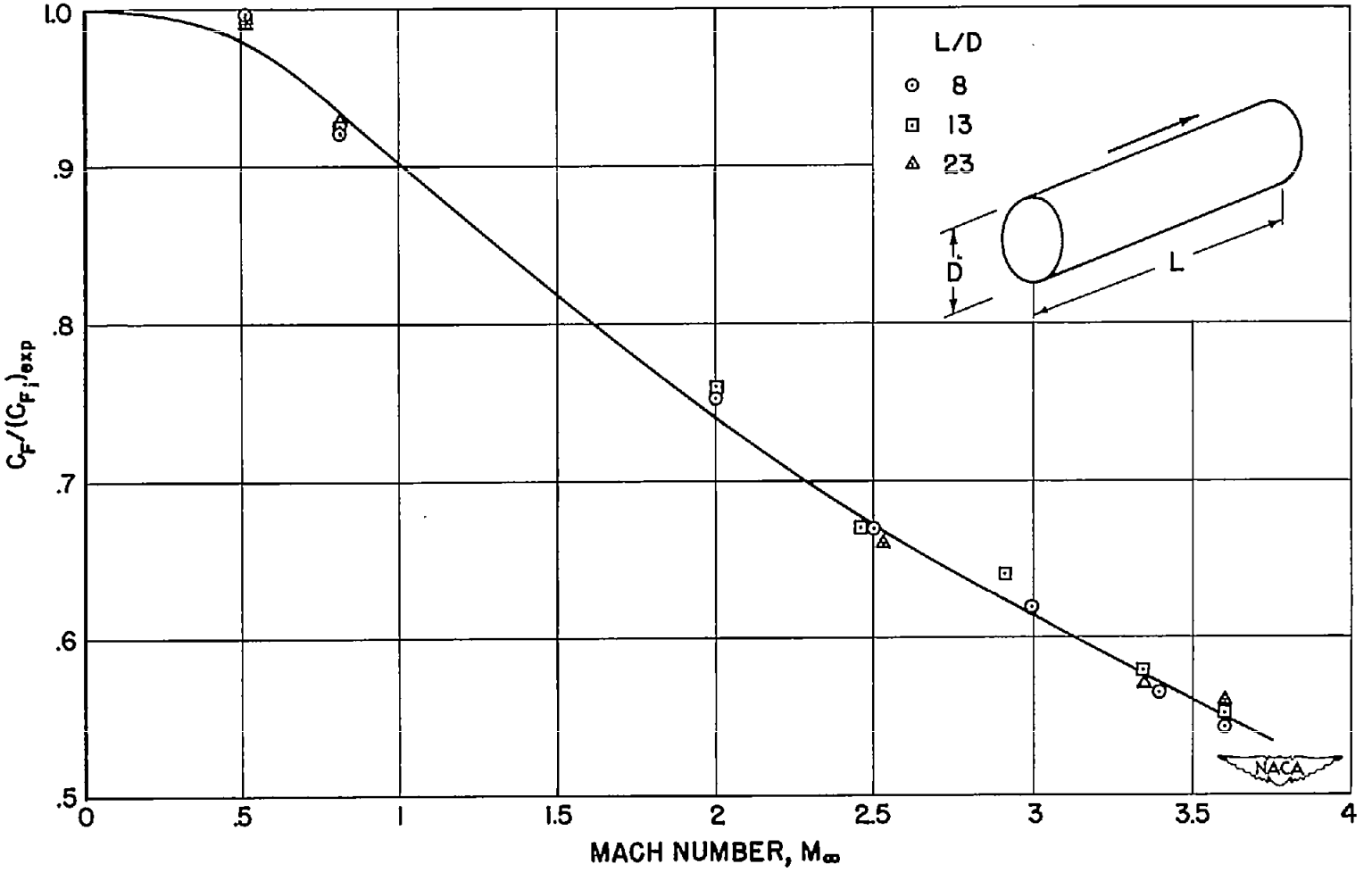

(c) Data of figure 17(b) referred to experimental C_{F_i}.

Figure 17.- Concluded.

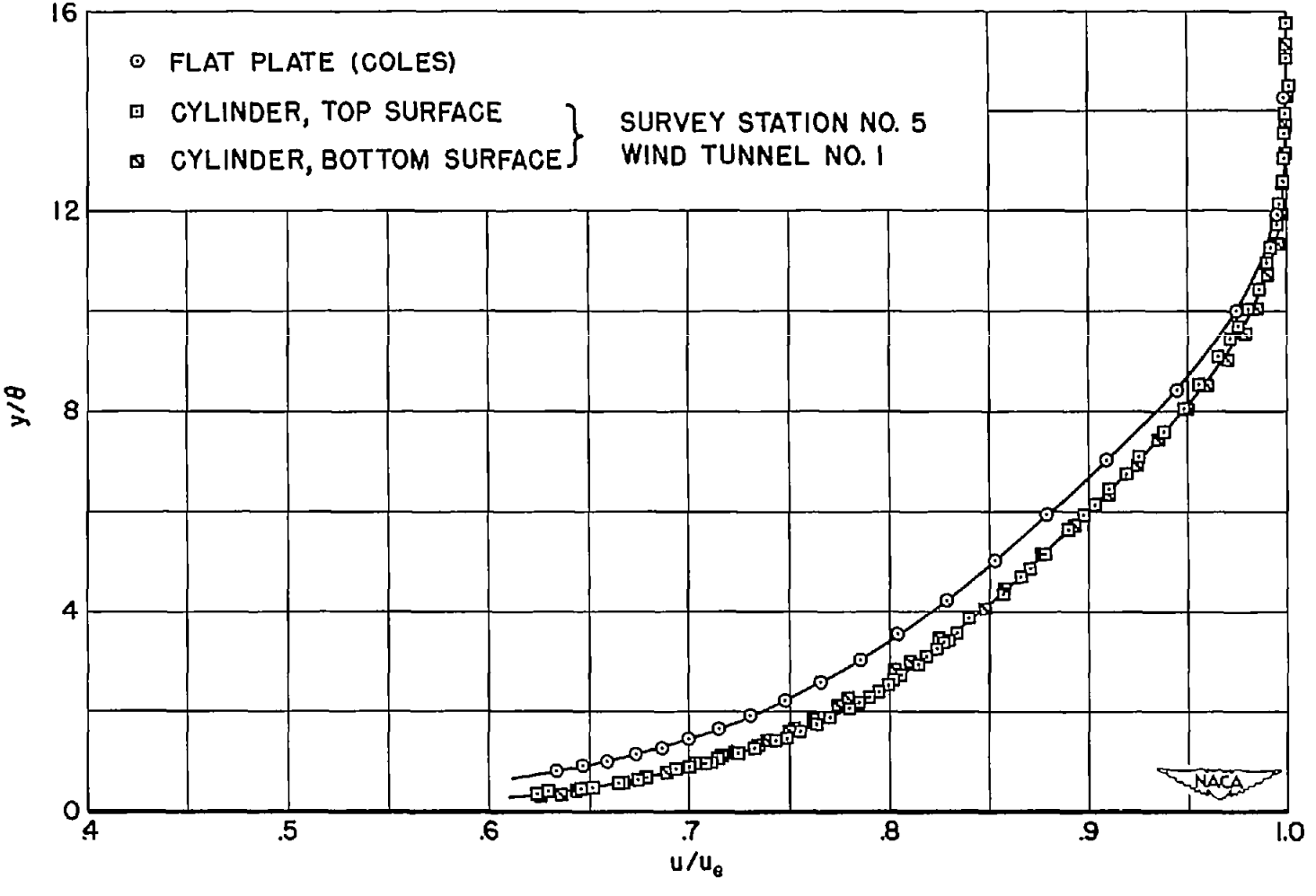

Figure 18.- Comparison of velocity profiles on cylinder and flat plate; M_∞=2.0, Re=6x10^6.

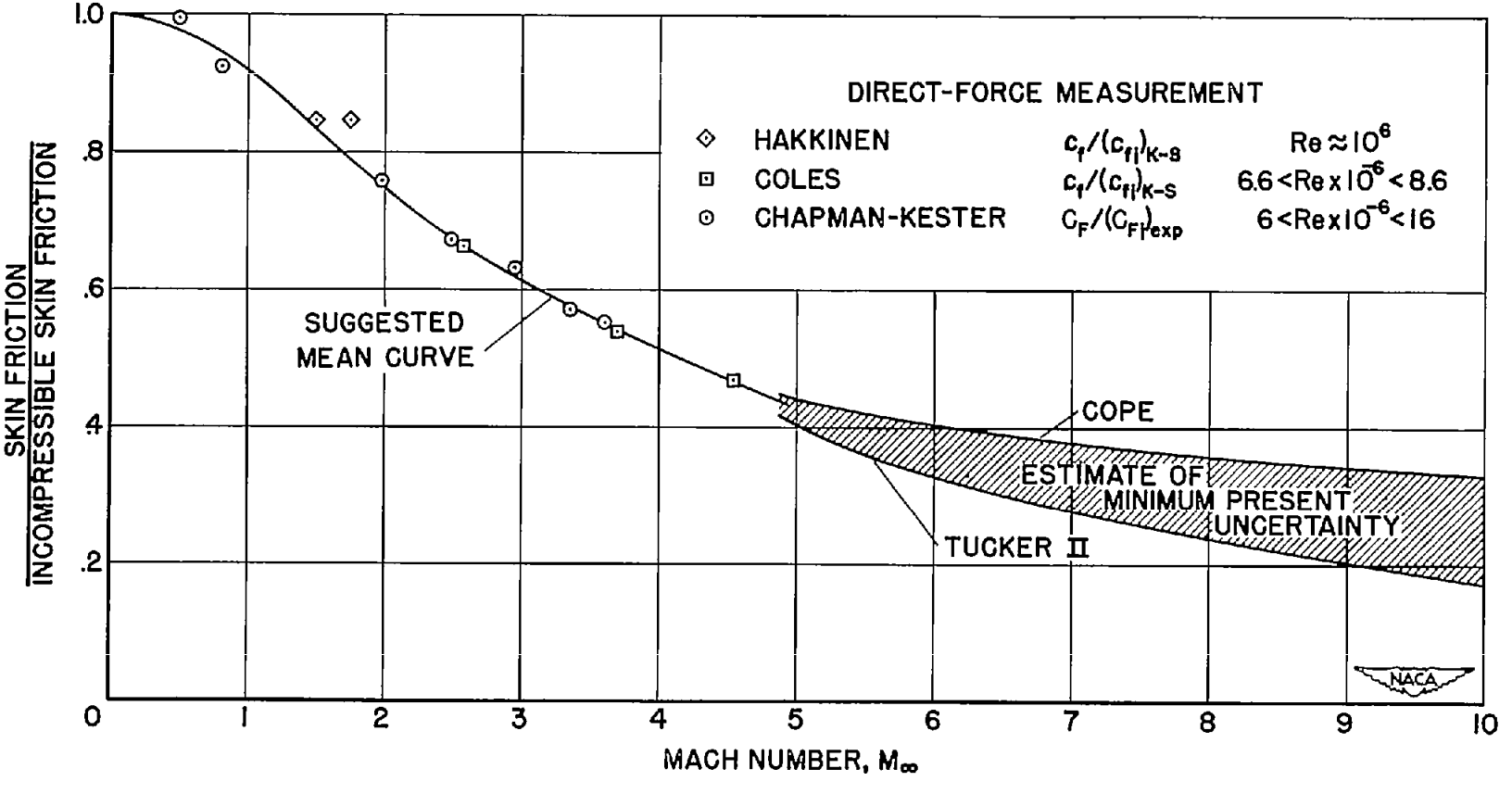

Figure 19.- Effect of Mach number on turbulent skin friction obtained by direct-force method for constant pressure and no heat transfer.

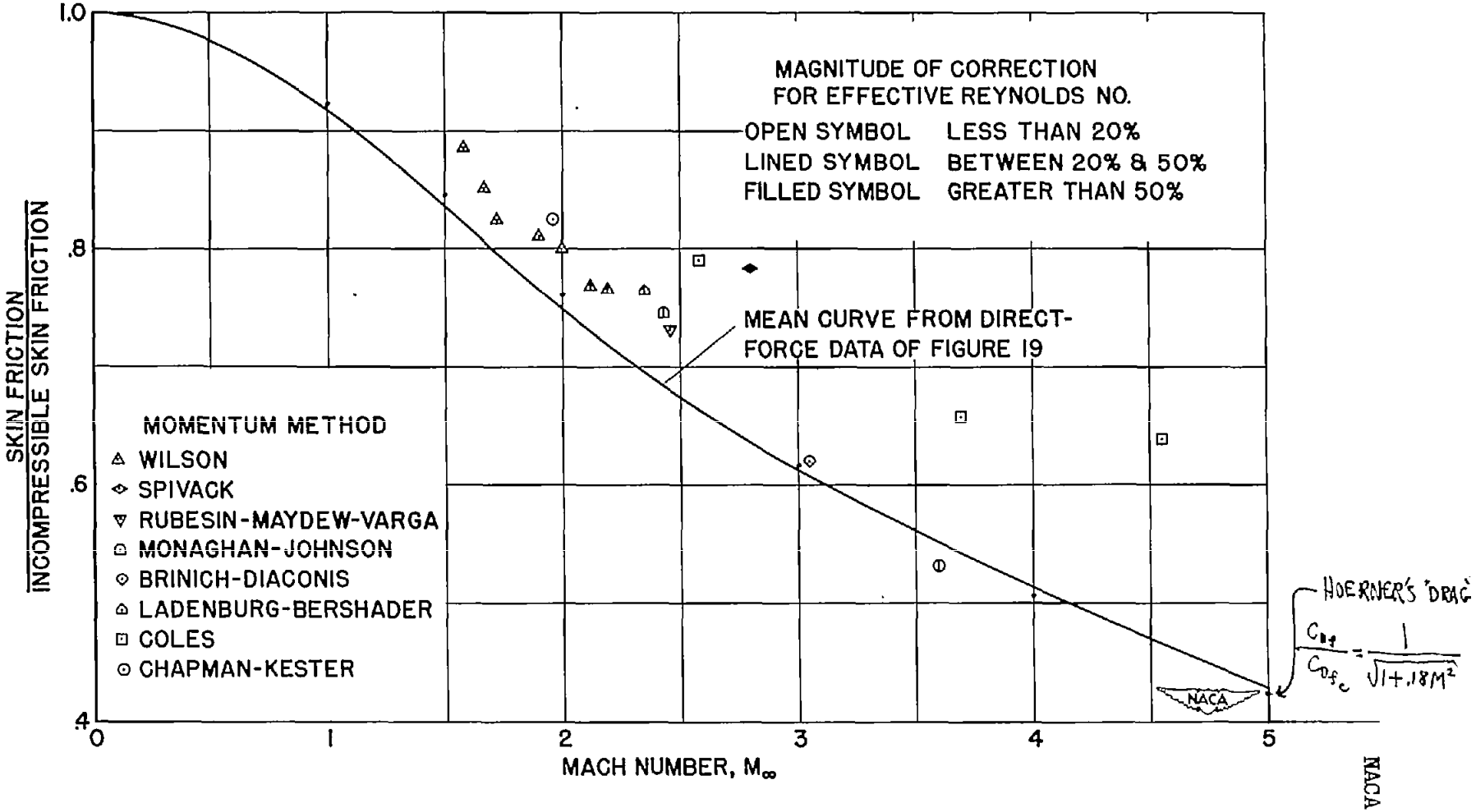

Figure 20.- Comparison of average skin-friction determinations from momentum method with those obtained from direct-force method.

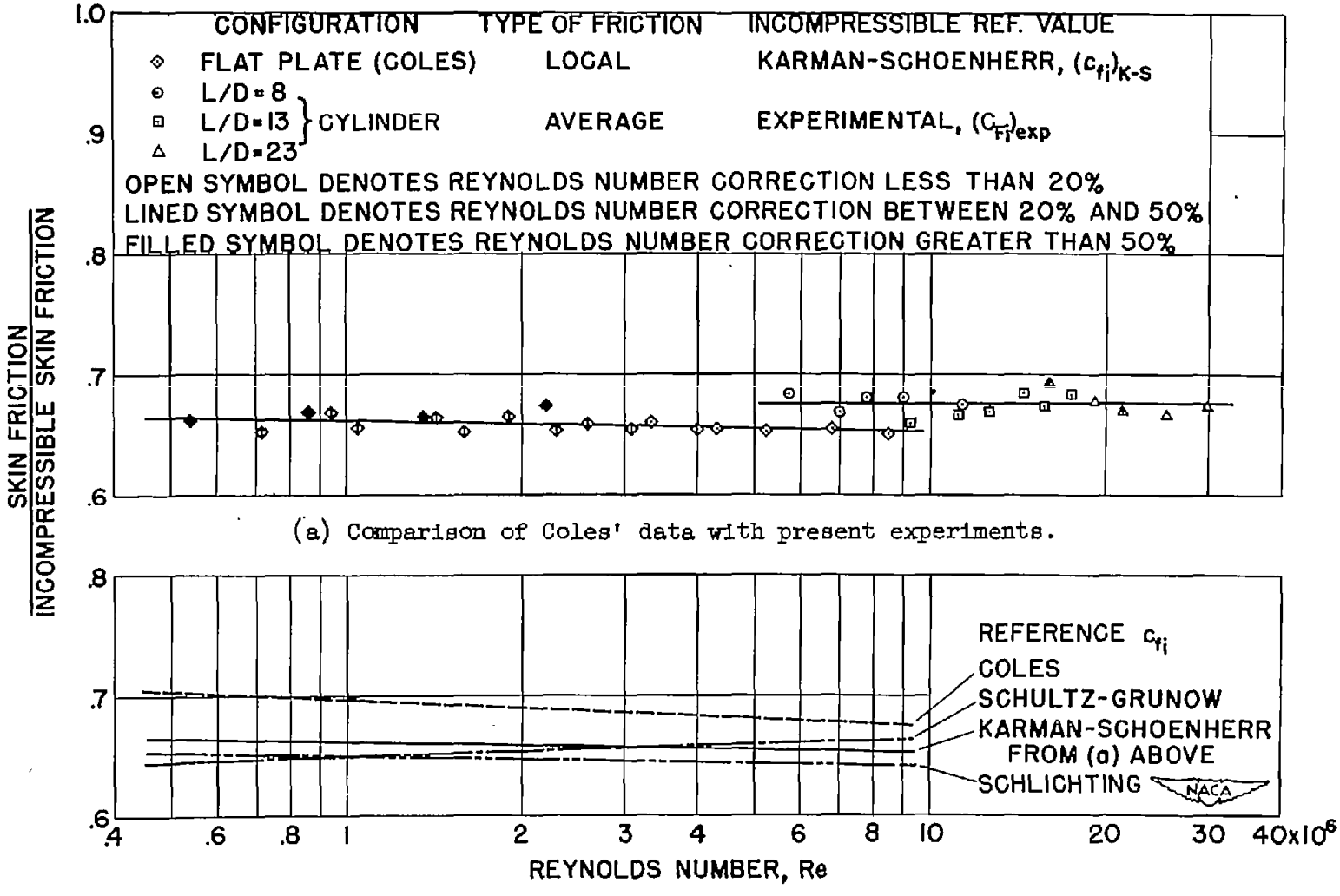

(a) Comparison of Coles' data with present experiments.

(b) Coles' data referred to various c_{f_i}.

Figure 21.- Effect of Reynolds number on ratio of compressible to incompressible skin friction; $M_\infty = 2.50$.